© 2021. Published by The Company of Biologists Ltd | Development (2021) 148, dev192443. doi:10.1242/dev.192443

RESEARCH ARTICLE

# Feedback control of the Gpr161-$G_{\alpha s}$-PKA axis contributes to basal Hedgehog repression in zebrafish

**Philipp M. Tschaikner[1,2], Dominik Regele[1], Ruth Röck[2], Willi Salvenmoser[3], Dirk Meyer[1], Michel Bouvier[4], Stephan Geley[5], Eduard Stefan[2,‡] and Pia Aanstad[1,*,‡]**

## ABSTRACT

Hedgehog (Hh) ligands act as morphogens to direct patterning and proliferation during embryonic development. Protein kinase A (PKA) is a central negative regulator of Hh signalling, and in the absence of Hh ligands, PKA activity prevents inappropriate expression of Hh target genes. The orphan G-protein-coupled receptor Gpr161 contributes to the basal Hh repression machinery by activating PKA. Gpr161 acts as an A-kinase-anchoring protein, and is itself phosphorylated by PKA, but the functional significance of PKA phosphorylation of Gpr161 in the context of Hh signalling remains unknown. Here, we show that loss of Gpr161 in zebrafish leads to constitutive activation of medium and low, but not maximal, levels of Hh target gene expression. Furthermore, we find that PKA phosphorylation-deficient forms of Gpr161, which we show directly couple to $G_{\alpha s}$, display an increased sensitivity to Shh, resulting in excess high-level Hh signalling. Our results suggest that PKA feedback-mediated phosphorylation of Gpr161 may provide a mechanism for fine-tuning Gpr161 ciliary localisation and PKA activity.

**KEY WORDS: Hedgehog signalling, Gpr161, PKA, Cilia, Zebrafish**

## INTRODUCTION

The Hh signalling pathway is a key regulator of cell fate specification and proliferation during embryonic development, and plays important roles in adult tissue homeostasis (Briscoe and Thérond, 2013; Ingham et al., 2011). Dysregulation of Hh signalling can lead to the formation of common and severe forms of human cancers such as basal cell carcinoma and medulloblastoma (Jiang and Hui, 2008; Raleigh and Reiter, 2019).

When Hh ligands bind their receptor Patched (Ptch), the inhibition of Smo by Ptch is alleviated and Smo translocates to the primary cilium (Corbit et al., 2005), where it activates downstream signalling to regulate the activity of the bifunctional Gli transcription factors.

Hh ligands act as morphogens, and the transcriptional outcome of Hh signalling is determined by the balance between repressor and activator forms of the Gli transcription factors. This balance is controlled by the activity of PKA and other kinases (Hui and Angers, 2011; Niewiadomski et al., 2019). In the absence of Hh, the basal Hh repression machinery maintains a high level of PKA activity. PKA phosphorylates the Gli proteins, and primes them for further phosphorylation and proteolytic cleavage to yield truncated forms that act as transcriptional repressors (GliR) (Niewiadomski et al., 2014; Pan et al., 2009; Wang et al., 2000). In addition, PKA also plays a role in restricting the activity of full-length Gli (GliA) by promoting its association with Sufu (Humke et al., 2010; Marks and Kalderon, 2011). Low levels of exposure to Hh ligands block the formation of GliR, whereas high levels of Hh exposure are required for the formation of the activator forms of Gli. This is thought to be controlled through a cluster of six PKA target residues in Gli, with distinct phosphorylation patterns regulating the formation of repressor and activator forms (Niewiadomski et al., 2014). This rheostat mechanism ensures that the level of Gli transcriptional activity corresponds to the level of PKA activity, which in turn must be controlled by the level of Smo activity and Hh ligand exposure (Niewiadomski et al., 2014, 2019). Consistent with this, a complete loss of PKA activity leads to constitutive (Smo independent) maximal Hh signalling, whereas constitutive activation of PKA abolishes all Hh-dependent transcription (Hammerschmidt et al., 1996; Tuson et al., 2011; Zhao et al., 2016).

A central and long-standing question in Hh signalling regards the nature of the basal repression machinery and the mechanism of its regulation. In *Drosophila*, Smo has been shown to regulate PKA activity directly by activating $G_{\alpha i}$ proteins to modulate cAMP levels (Ogden et al., 2008). Although vertebrate Smo can also couple to $G_{\alpha i}$ (Riobo et al., 2006), it is clear that $G_{\alpha i}$ is not required for all aspects of vertebrate Hh signalling (Ayers and Thérond, 2010), raising the question of which other mechanisms contribute to the regulation of PKA?

The murine orphan G-protein-coupled receptor (GPCR) Gpr161 contributes to basal Hh repression by activating $G_{\alpha s}$ and consequently PKA (Mukhopadhyay et al., 2013). In the absence of Hh ligands, Gpr161 localises to the primary cilia, and is removed from the cilia upon activation of Smo (Mukhopadhyay et al., 2013; Pal et al., 2016). These results suggest that Gpr161 maintains PKA activity in the cilium in the absence of Hh, and that the ciliary exit of Gpr161 is required for Hh signalling and the reduction of PKA activity (Mukhopadhyay et al., 2013; Pal et al., 2016). However, Gpr161 has also been shown to be a substrate of PKA, and can act as an A kinase anchoring protein (AKAP) (Bachmann et al., 2016; Torres-Quesada et al., 2017; Tschaikner et al., 2020). Thus, the exact molecular mechanisms that regulate Gpr161 activity in the context of Hh signalling remain unclear.

Murine Gpr161 mutants display severe developmental malformations, including craniofacial defects and ventralisation of the neural tube, that are independent of Smo function, suggesting that loss of Gpr161 function causes constitutive activation of downstream

[1]Institute of Molecular Biology and Center for Molecular Biosciences, University of Innsbruck, Innsbruck 6020, Austria. [2]Institute of Biochemistry and Center for Molecular Biosciences, University of Innsbruck, Innsbruck 6020, Austria. [3]Institute of Zoology and Center of Molecular Bioscience Innsbruck, University of Innsbruck, Innsbruck 6020, Austria. [4]Institute for Research in Immunology and Cancer (IRIC), Université de Montréal, Montreal, QC H3T 1J4, Canada. [5]Division of Molecular Pathophysiology, Medical University of Innsbruck, Innsbruck 6020, Austria.
*Present address: Research Department of Genetics, Evolution and Environment, University College London, Gower St, London WC1E 6BT, UK.

‡Authors for correspondence (p.aanstad@ucl.ac.uk; eduard.stefan@uibk.ac.at)

M.B., 0000-0003-1128-0100; S.G., 0000-0002-3169-5322; P.A., 0000-0003-3893-2973

**Handling Editor: James Briscoe**
**Received 4 May 2020; Accepted 14 January 2021**

Development (2021) 148, dev192443. doi:10.1242/dev.192443

Hh signal transduction (Mukhopadhyay et al., 2013). However, the neural tube of Gpr161 mutants is less severely ventralised than that observed in embryos completely lacking PKA activity (Tuson et al., 2011). In murine neural progenitor cells (NPCs), Gpr161 has been found to be epistatic to Smo for only low-level signalling, whereas expression of high-level targets, such as Nkx2.2 and FoxA2, still depend on Smo function (Pusapati et al., 2018), suggesting that in the neural tube, Gpr161 plays an important role in controlling basal and low-level Hh signalling activity. In murine NIH 3T3 fibroblasts, loss of Gpr161 does not affect basal repression, although the mutant cells display an increased sensitivity to Hh ligands. Taken together, these results suggest that additional $G_{\alpha s}$-coupled receptors may be involved in maintaining PKA activity in the absence of Hh ligands (Pusapati et al., 2018). Supporting this, several studies have identified additional GPCRs that regulate Hh signalling in parallel with or downstream of Smo (Klein et al., 2001; Singh et al., 2015; Stückemann et al., 2012; Yatsuzuka et al., 2019).

To facilitate the study of Gpr161 in Hh signalling, we have generated and characterised zebrafish *gpr161* mutants, and show that Gpr161 is an important negative modulator of Hh signalling in zebrafish. Complete loss of Gpr161 function leads to constitutive, Smo-independent activation of low-to-medium-level Hh target genes, whereas the expression of maximal-level Hh targets still depends on Smo in *gpr161* mutants. We also show that PKA phosphorylation of Gpr161 regulates the dynamics of ciliary localisation of Gpr161, and propose that this may be important for the fine-tuning of high-level Hh signalling.

## RESULTS

### Gpr161 is an evolutionarily conserved GPCR with two paralogs in zebrafish

The zebrafish genome contains two conserved paralogues of Gpr161, Gpr161a (ENSDART00000151311.2) and Gpr161b (ENSDART00000078051.6), with 71% sequence identity and 84% sequence similarity between each other, and more than 70% similarity to the murine Gpr161 protein (Fig. S1). Expression analysis using qRT-PCR showed that both transcripts are expressed during embryonic development, but while *gpr161b* is maternally provided, *gpr161a* expression is first detected at 9 h post fertilisation (hpf) (Fig. 1A). In mouse, Gpr161 localises to primary cilia, and this localisation has been proposed to be important for its role in modulating the Hh signalling pathway (Mukhopadhyay et al., 2013; Pal et al., 2016; Shimada et al., 2018). To test whether zebrafish Gpr161 also localise to primary cilia, we injected mRNA of Myc-tagged versions of Gpr161a and Gpr161b into one-cell stage zebrafish embryos. Both Gpr161a and Gpr161b were readily detected at primary cilia in zebrafish embryos (Fig. 1B).

### Gpr161a and Gpr161b are functionally redundant but essential during zebrafish embryonic development

To investigate the functional roles of Gpr161a and Gpr161b during zebrafish development, we used CRISPR/Cas9 to generate mutant alleles for each gene, $gpr161a^{ml200}$, which carries a 6 bp out of frame insertion in the second coding exon of *gpr161a*, and $gpr161b^{ml201}$, harbouring an 8 bp deletion in the second coding exon of *gpr161b*. Both alleles introduce a premature stop codon within the seven-transmembrane-domain region of the respective proteins, and are predicted to be functionally inactive (Fig. S2). Animals homozygous for either $gpr161a^{ml200}$ or $gpr161b^{ml201}$ alone, or animals lacking three of the four *gpr161* alleles, showed no effect either on embryonic development or in adult viability and fertility. In contrast, *gpr161a; gpr161b* double zygotic homozygous mutant embryos showed clear morphological phenotypes by 24 hpf, suggesting that Gpr161a and Gpr161b act in a functionally redundant manner (data not shown). To determine the contribution of maternal Gpr161b, we generated embryos from incrosses of $gpr161b^{-/-}$; $gpr161a^{+/-}$ animals. Quantitative analysis of *gpr161a* expression at the two-cell stage of *MZgpr161b; gpr161a* mutant embryos showed that a complete loss of Gpr161b did not result in a compensatory maternal upregulation of Gpr161a (Fig. S3). We conclude that $MZgpr161b^{-/-}$; $gpr161a^{-/-}$ mutant embryos are likely to represent a complete loss of function of zebrafish Gpr161, and refer to these mutants as *gpr161* mutants below.

At 24 hpf, *gpr161* mutant embryos display several developmental abnormalities, including malformed eyes lacking any obvious lens or retinal structure (Fig. 1C). At this stage of development, wild-type embryos display chevron-shaped somites, whereas the somites of *gpr161* mutants have a more obtuse angle (Fig. 1C). These phenotypes, which are present in the double mutant line, but not in $MZgpr161b^{-/-}$; $gpr161a^{+/-}$ or $gpr161b^{+/-}$; $gpr161a^{-/-}$ embryos, are similar to those observed in $ptch1^{-/-}$; $ptch2^{-/-}$ double mutant embryos (Koudijs et al., 2008). However, in contrast to $ptch1^{-/-}$; $ptch2^{-/-}$ double mutant embryos, which lack eyes (Koudijs et al., 2008), a rudimentary eye can be identified in *gpr161* mutants at 72 hpf (Fig. 1D,F).

At this stage, the retina of wild-type embryos is organised into six evolutionarily conserved layers: the pigmented epithelium, the photoreceptor cell layer, the outer plexiform layer, the inner nuclear layer, the inner plexiform layer and the ganglion cell layer (Schmitt and Dowling, 1999). Semi-thin sectioning revealed that, although eye morphogenesis was abnormal, remnants of all six layers were clearly identified by morphology (Fig. 1F, Fig. S4A). However, these layers are not well separated and the optic cup is partially folded (Fig. S4B). Additionally, remnants of a forming lens can be found in *gpr161* mutant embryos (Fig. S4A). A striking phenotype of the *gpr161* mutants is the open pharynx and an apparent complete loss of jaw structures, as demonstrated by scanning electron microscopy (SEM) imaging. However, remnants of mandibulary and maxillary cartilage are still detectable in transverse semi-thin sections (Fig. 1E, data not shown). Although $ptch1^{-/-}$; $ptch2^{-/-}$ double mutant embryos were reported to lack all olfactory structures (Koudijs et al., 2008), scanning electron microscopy imaging revealed that in the *gpr161* mutants the olfactory pits are present, although severely reduced in size (Fig. 1E).

Zebrafish embryos with a strong Hh gain-of-function phenotype, such as the $ptch1^{-/-}$; $ptch2^{-/-}$ double mutants, also display defects in the development of the otic vesicles (Koudijs et al., 2008). The *gpr161* mutant embryos exhibited smaller otic vesicles compared with wild-type embryos (Fig. 1D). Serial sections of the otic vesicles revealed the absence of the dorsolateral septum (Fig. S4C). The combination of developmental defects in ocular and otic structures is commonly seen in mutants of negative regulators of Hh signalling, such as *sufu*, *ptch1* and *hhip* (Whitfield et al., 1996), and suggests that Gpr161 also acts to negatively regulate Hh signalling in zebrafish.

Gpr161 mutant mice do not form limb buds (Hwang et al., 2018; Mukhopadhyay et al., 2013), and $ptch1^{-/-}$; $ptch2^{-/-}$ double mutant zebrafish embryos lack pectoral fin buds (Koudijs et al., 2008). In contrast to the requirement for Gpr161 in murine limb formation, pectoral fin formation appeared normal in the zebrafish *gpr161* mutant embryos (Fig. 1D, Fig. S4D).

A previous study using morpholinos to knock down Gpr161b function reported a role for zebrafish Gpr161 in left-right axis specification during early development (Leung et al., 2008). We

Development (2021) 148, dev192443. doi:10.1242/dev.192443

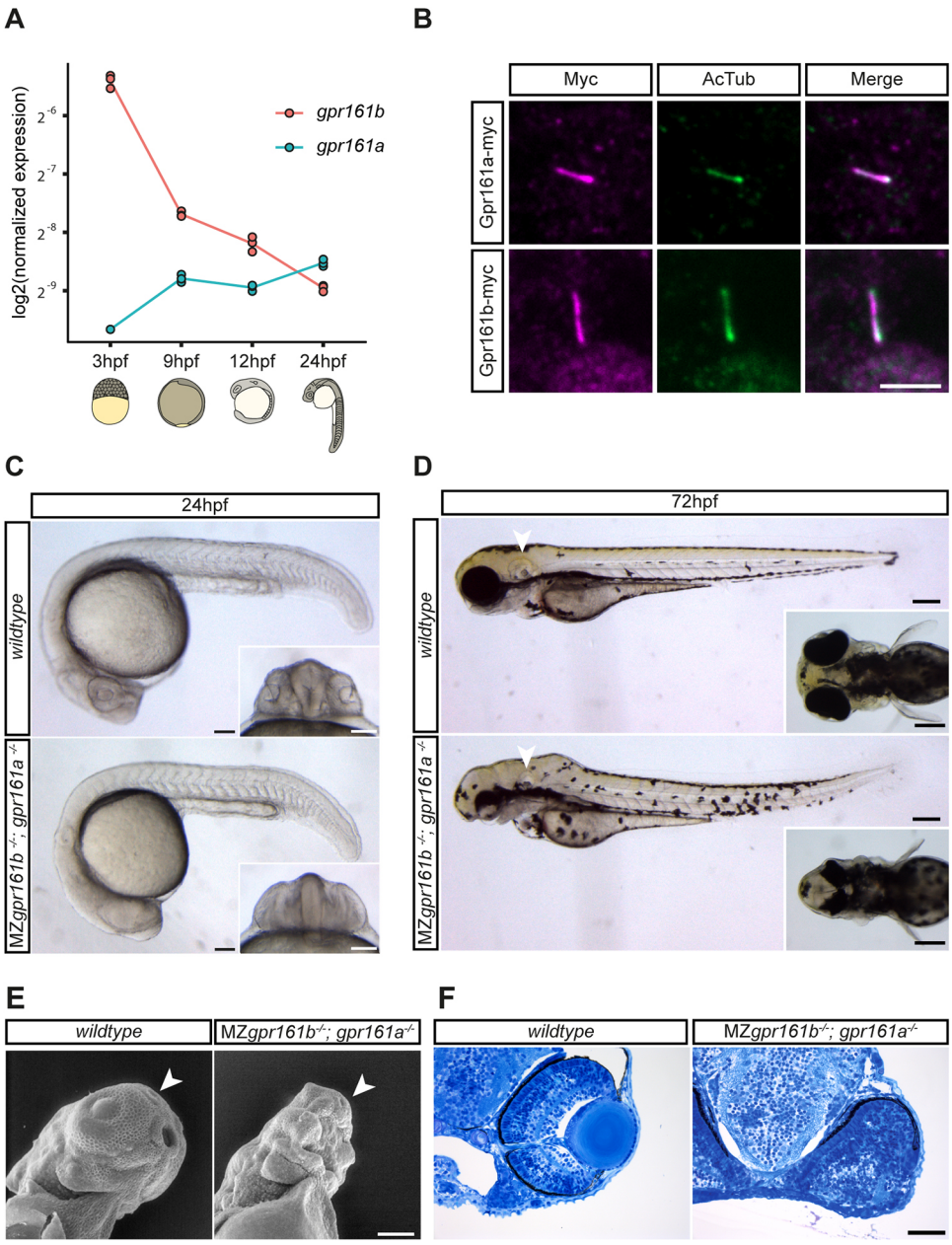


**Fig. 1. Gpr161 is an evolutionarily conserved ciliary GPCR that is essential during embryonic development.**
(A) *gpr161a* and *gpr161b* transcript levels at different stages of development analysed in whole-embryo lysates in triplicate using RT-qPCR. (B) Wild-type embryos were injected with *gpr161a-myc* or *gpr161b-myc* mRNA at the one-cell stage and fixed at 9 hpf before immunostaining for acetylated tubulin (AcTub; purple), a marker for the ciliary axoneme, and Myc (green). Scale bar: 5 µm. (C) Lateral views of wild-type and MZ*gpr161b*$^{-/-}$; *gpr161a*$^{-/-}$ embryos at 24 hpf. Insets show ventral views of the developing eyes; arrowheads indicate the otic vesicle. Scale bars: 100 µm. (D) Wild-type and MZ*gpr161b*$^{-/-}$; *gpr161a*$^{-/-}$ embryos at 72 hpf. Arrowheads indicate otic vesicle. Scale bars: 200 µm. Insets show a dorsal view of the head. (E) Ventrolateral views of the craniofacial region of wild-type and MZ*gpr161b*$^{-/-}$; *gpr161a*$^{-/-}$ embryos at 72 hpf taken by scanning electron microscopy; arrowheads indicate the olfactory pit. Scale bar: 100 µm. (F) Transverse semi-thin sections of the eye in wild-type and MZ*gpr161b*$^{-/-}$; *gpr161a*$^{-/-}$ embryos fixed at 72 hpf (Richardson staining). Scale bar: 50 µm.

assessed laterality defects in the *gpr161* mutants using *in situ* hybridisation for the myocardial marker *cardiac myosin light chain 2* (*cmlc2*) (Yelon et al., 1999). At 24 hpf, the myocardium shows clear laterality, with the heart tube jogging to the left (Fig. S5) in 100% of both wild-type (30/30 embryos in two independent experiments) and *gpr161* mutant (16/16 embryos in two independent experiments) embryos, suggesting that loss of Gpr161 does not affect left-right axis specification in zebrafish, and that the laterality defects observed in the Gpr161b morphants may be due to the well-documented off-target effect of morpholino treatment (Kok et al., 2015; Lai et al., 2019; Schulte-Merker and Stainier, 2014).

### Hedgehog signalling is upregulated in *gpr161* mutant embryos

The morphological phenotypes observed in *gpr161* mutants are consistent with increased Hh signalling. To determine whether Hh signalling is upregulated in *gpr161* mutants, we assessed the expression of known Hh target genes in the neural tube by qRT-PCR and RNA *in situ* hybridisation (Fig. 2A,B). The Hh target genes *ptch2*, *gli1*, *nkx2.2b* and *nkx6.1* (Fig. 2B) were all strongly upregulated, whereas *pax7a*, which is repressed by Hh signalling (Guner and Karlstrom, 2007), was strongly downregulated in *gpr161* mutant compared with wild-type embryos (Fig. 2B). RNA *in situ* hybridisation revealed that expression of *shha*, the major Hh ligand expressed in the neural plate, was unchanged in *gpr161* mutants (Fig. 2A). However, expression of *ptch2*, a direct transcriptional target of Hh signalling (Concordet et al., 1996), was expanded in *gpr161* mutants (Fig. 2A), suggesting that Hh signalling is upregulated in *gpr161* mutants downstream of Shh expression. Similarly, expression of *olig2*, a marker of motor neuron induction that depends on low-level Hh activity (Dessaud et al., 2007; Park et al., 2002), as well as *nkx2.2a*, a marker for V3 interneuron progenitor cells of the lateral floorplate (Barth and Wilson, 1995; Briscoe et al., 1999), were clearly expanded in the *gpr161* mutant neural tube (Fig. 2A). We note that the expansion of the low-level target *olig2* appears to be stronger than the expansion of the

Development (2021) 148, dev192443. doi:10.1242/dev.192443

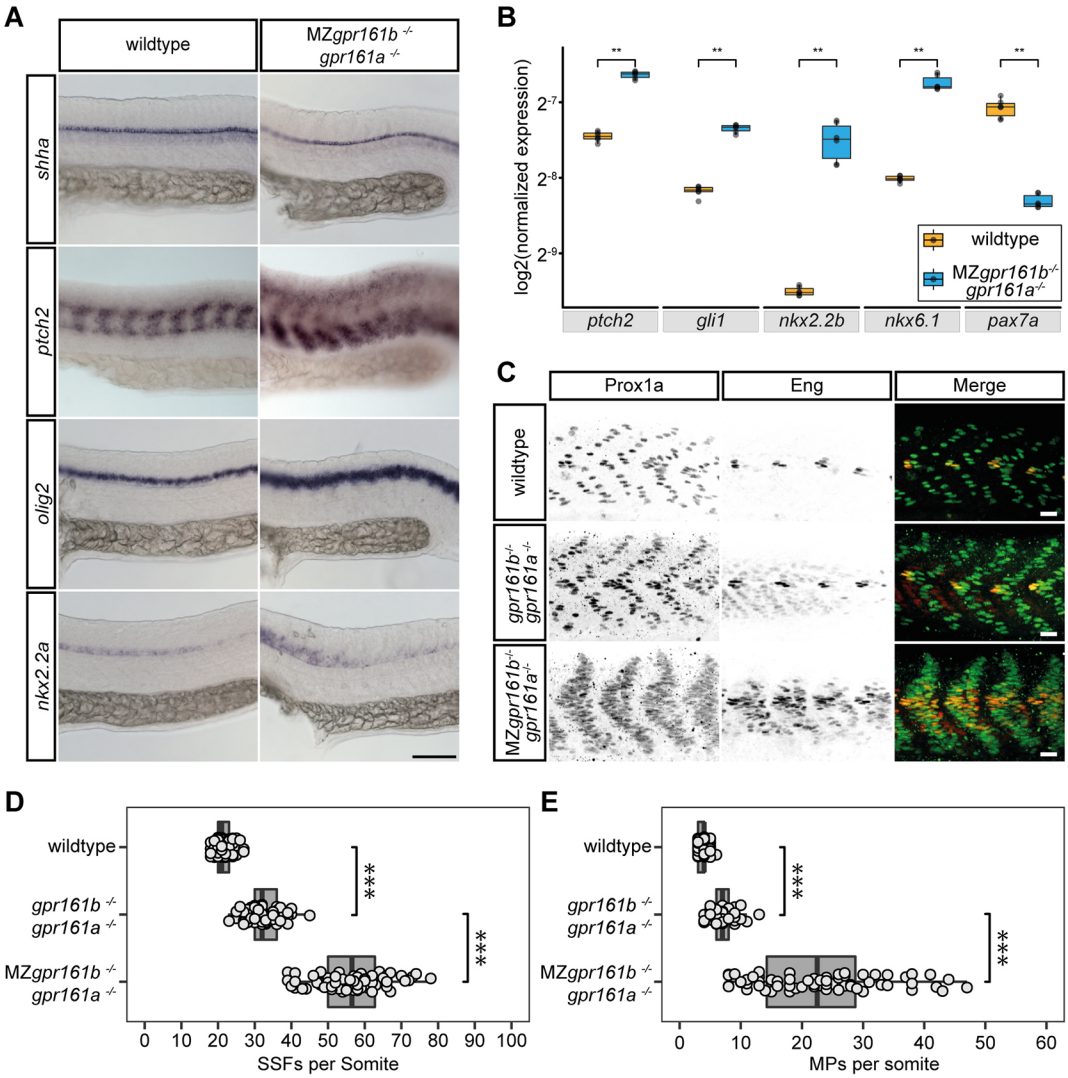


**Fig. 2. Hh signalling activity is increased in *gpr161* mutants.** (A) RNA *in situ* hybridisation of *shha*, *ptch2*, *olig2* and *nkx2.2a* transcripts in wild-type and MZ*gpr161b*$^{-/-}$; *gpr161a*$^{-/-}$ embryos fixed at 24 hpf (lateral view). Scale bar: 100 µm. (B) Transcript levels of *ptch2*, *gli1*, *nkx2.2b*, *nkx6.1* and *pax7a* in wild-type and MZ*gpr161b*$^{-/-}$; *gpr161a*$^{-/-}$ embryos at 24 hpf determined by RT-qPCR ($n$=3; **$P$<0.01, Kruskal–Wallis rank sum test, Dunn's post-hoc test for multiple comparisons). (C) Immunostaining of Prox1 and Eng proteins in 24 hpf zebrafish embryos reveals the number of MPs (Prox1a/Eng double positive) as well as SFFs (Prox1 positive) in wild-type, *gpr161b*$^{-/-}$; *gpr161a*$^{-/-}$ and MZ*gpr161b*$^{-/-}$; *gpr161*$^{-/-}$ embryos fixed at 24 hpf. Scale bars: 20 µm. (D,E) Number of (D) SSFs and (E) MPs per somite in wild-type ($n$=93 somites in 22 embryos), *gpr161b*$^{-/-}$; *gpr161a*$^{-/-}$ ($n$=60 somites in 20 embryos) and MZ*gpr161b*$^{-/-}$; *gpr161a*$^{-/-}$ ($n$=66 somites in 22 embryos) embryos fixed at 24 hpf. ***$P$<0.001 (one-way ANOVA, Tukey's post-hoc test for pairwise comparisons). Box plots show median values (centre lines) and the interquartile ranges (boxes); whiskers extend to the highest and lowest values within 1.5×IQR (inter-quartile range).

high-level target *nkx2.2a* (Fig. 2A). Taken together, these results show that loss of Gpr161 leads to a derepression of the Hh signalling pathway in zebrafish.

In the zebrafish myotome, sustained Hh signalling during gastrulation and somitogenesis stages have been shown to be required for the specification of several cell types, including Prox1 and Eng double-positive muscle pioneer cells (MPs) and Prox1-positive superficial slow fibres (SSFs) (Wolff et al., 2003). Although medium-to-low-level Hh signalling is sufficient for the specification of SSFs, the formation of MPs requires higher levels of Hh (Wolff et al., 2003). Consistent with the expansion of Hh target genes in the neural tube, *gpr161* mutants also displayed an increase in both SSFs and MPs (Fig. 2C). Although zygotic Gpr161 loss of function resulted in a significant increase in both SSFs [from 22±2 (mean±s.d.) in wild type to 33±5 in zygotic *gpr161* mutants] and MPs [from 4±1 (mean±s.d.) in wild type to 7±2 in zygotic *gpr161* mutants], complete loss of both maternal and zygotic Gpr161 led to a stronger increase in both SSFs and MPs [56±9 (mean±s.d.) SSFs, and 23±10 MPs] (Fig. 2D,E), consistent with the requirement for sustained Hh signalling in muscle cell development (Wolff et al., 2003). These results suggest that, in the somites, loss of Gpr161 results in expansion of both high and low Hh signalling targets.

### Loss of Gpr161 leads to constitutive activation of medium and low, but not maximum, levels of Hh signalling

To determine whether Hh signalling is constitutively activated by loss of Gpr161, we used the zebrafish *smo* null allele *hi1640* (Chen et al., 2001) to generate zebrafish *gpr161b*$^{-/-}$; *gpr161a*$^{-/-}$; *smo*$^{-/-}$ triple mutants, and assessed Hh signalling activity using Prox1/Eng staining and neural tube markers, as above. Zebrafish *gpr161b*$^{-/-}$; *gpr161a*$^{-/-}$; *smo*$^{-/-}$ triple homozygous mutant embryos showed a morphological phenotype, an expansion of low-level target genes *ptch2* and *olig2*, as well as supernumerary SSFs and MPs, that were indistinguishable from *gpr161b*$^{-/-}$; *gpr161a*$^{-/-}$ double homozygous

Development (2021) 148, dev192443. doi:10.1242/dev.192443

mutant embryos (Fig. 3A-D, Fig. S6). In contrast to the *gpr161* double mutant, *gpr161b*$^{-/-}$; *gpr161a*$^{-/-}$; *smo*$^{-/-}$ triple mutant embryos showed no detectable *nkx2.2a* expression (Fig. 3D), suggesting that, in the neural tube, although not in the somites, high-level Hh target gene expression is dependent on Smo function in the absence of Gpr161. However, it is unclear whether the myotomal MPs represent the outcome of maximal Hh levels, similar to *nkx2.2a* expression in the neural tube. Previous studies have shown that Hh

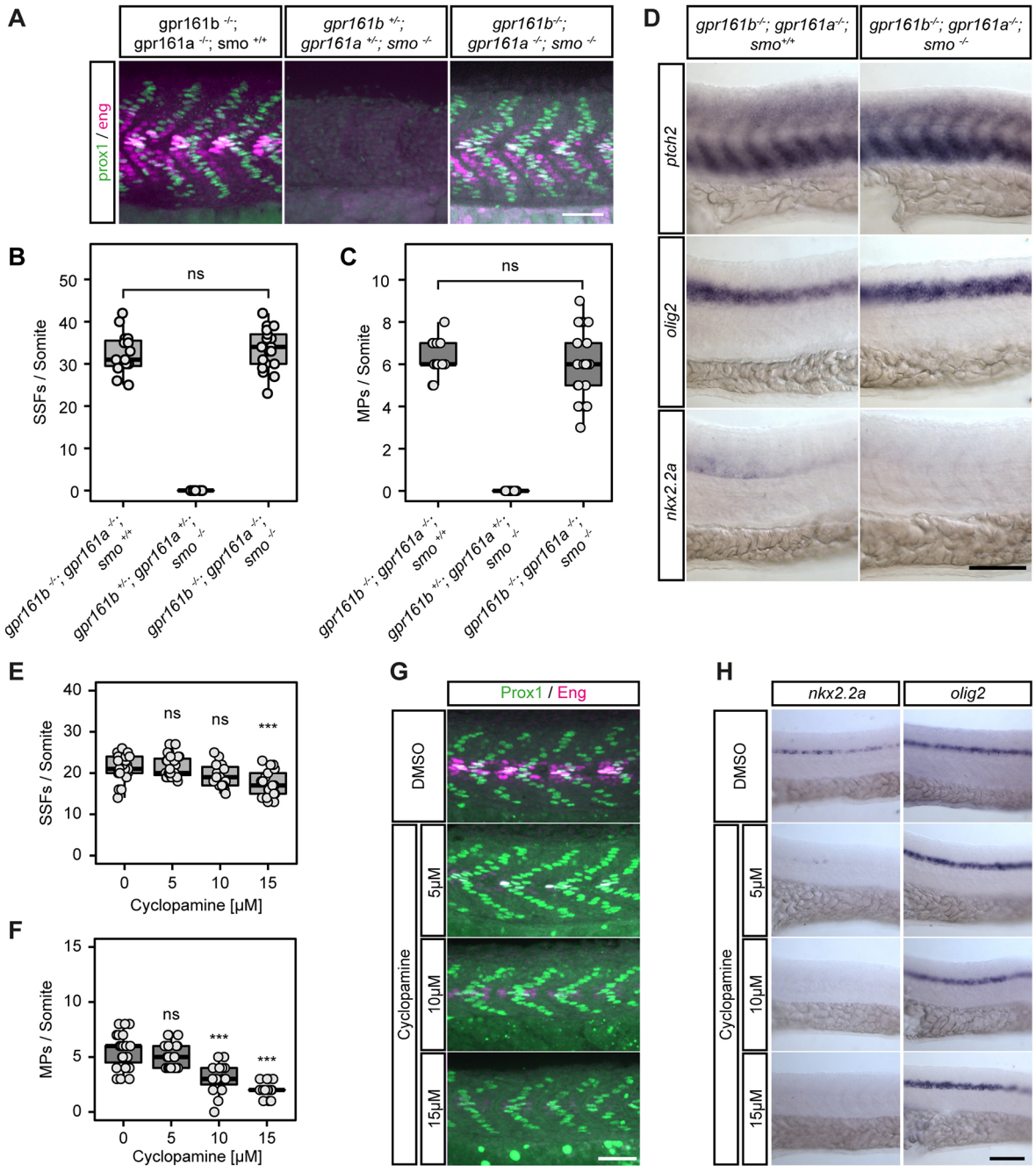


**Fig. 3. Constitutive activation of low- and medium- but not high-level Hh targets in *gpr161* mutants.** (A) Prox1 (green)/Eng (purple) immunostaining of mutant embryos at 24 hpf. Scale bar: 50 µm. (B,C) Quantification of SSFs and MPs from experiments presented in A (*gpr161b*$^{-/-}$; *gpr161a*$^{-/-}$; *smo*$^{+/+}$ and *gpr161b*$^{+/-}$; *gpr161a*$^{+/-}$; *smo*$^{-/-}$: *n*=15 somites in five embryos; *gpr161b*$^{-/-}$; *gpr161a*$^{-/-}$; *smo*$^{-/-}$: *n*=21 somites in seven embryos; all others: *n*=27 somites in nine embryos; ns, not significant; one-way ANOVA, Tukey's post-hoc test for pairwise comparisons). (D) RNA *in situ* hybridisation of *ptch2*, *olig2* and *nkx2.2a* transcripts in *gpr161b*$^{-/-}$; *gpr161a*$^{-/-}$; *smo*$^{+/+}$ and *gpr161b*$^{-/-}$; *gpr161a*$^{-/-}$; *smo*$^{-/-}$embryos fixed at 24 hpf (lateral view). Scale bar: 100 µm. (E,F) Quantification of SSFs and MPs in wild-type embryos at 24 hpf after treatment with 0-15 µM cyclopamine (DMSO and 5 µM cyclopamine: *n*=27 somites in nine embryos; 10 µM cyclopamine: *n*=15 somites in five embryos; 15 mM cyclopamine: *n*=21 somites in seven embryos; ***$P$<0.001; ns, not significant; one-way ANOVA, Tukey's post-hoc test for pairwise comparisons). (G) Representative Prox1 (green)/Eng (purple) immunostaining of wild-type embryos at 24 hpf after treatment with 0-15 µM cyclopamine. Scale bar: 50 µm. (H) RNA *in situ* hybridisation of *nkx2.2a* and *olig2* transcripts in wild-type embryos at 24 hpf after treatment with 0-15 µM cyclopamine (lateral view). Scale bar: 100 µm. (A,C,G) The high levels of Eng (purple) staining in the *gpr161* double mutants (A) and DMSO-treated *gpr161* mutants (G) are due to Hh-dependent Eng-positive, Prox1-negative medial fast fibres, which are not included in the quantification (C). Box plots show median values (centre lines) and the interquartile ranges (boxes); whiskers extend to the highest and lowest values within 1.5×IQR (inter-quartile range).

Development (2021) 148, dev192443. doi:10.1242/dev.192443

read-outs are exquisitely sensitive to the Smo antagonist cyclopamine (Wolff et al., 2003). We used low levels of cyclopamine to inhibit high-level Hh signalling, in order to compare the sensitivity of *nkx2.2a* expression and MP formation. Treatment with 5 µM cyclopamine is sufficient to strongly reduce *nkx2.2a* expression in the neural tube, but does not significantly affect MP or SSF formation in the myotome (Fig. 3E-H). At 10 and 15 µM, cyclopamine abolishes *nkx2.2a* expression, and the numbers of MPs are strongly reduced. With 15 µM cyclopamine, there is also a small but significant reduction in the number of SSFs (Fig. 3E). These results suggest that, whereas *nkx2.2a* is a target of high-to-maximal Hh signalling, MPs require a lower level of Hh for their specification. Taken together, these results suggest that, in zebrafish, loss of Gpr161 leads to constitutive Smo-independent activation of all but the very highest levels of Hh signalling. Supporting this idea, injection of *shh* mRNA to activate Hh signalling in the *gpr161* mutants resulted in an expansion of *nkx2.2a* expression, and in an increase in the number of MPs, but did not further increase the number of SSFs (Fig. S7).

### Activation of PKA rescues *gpr161* mutant phenotypes

Murine Gpr161 is proposed to act as a $G_{\alpha s}$-coupled receptor, which contributes to maintain basal levels of PKA activity to keep the Hh pathway inactive (Mukhopadhyay et al., 2013). To confirm this, we used a bioluminescence resonance energy transfer (BRET) sensor to monitor $G_{\alpha s}$ activation (Thomsen et al., 2016), as well as a cellular PKA biosensor based on a *Renilla* luciferase (Rluc) protein fragment complementation assay (PCA) (Röck et al., 2019; Stefan et al., 2007, 2011) (Fig. S9B). The $G_{\alpha s}$-RLucII/$\gamma_1$-GFP10 BRET assay measures the interaction between the α subunit, tagged with RLuc, and the βγ subunits, tagged with GFP10, where dissociation of the α subunit from the βγ subunits (resulting in reduced BRET) corresponds to the activation of the $G_{\alpha s}$ subunit (Thomsen et al., 2016, see also Fig. S9A). Co-expression of Gpr161 and the components of the Gαβγ BRET reporter resulted in a reduction of the $G_{\alpha s}$-RLucII/$\gamma_1$-GFP10 BRET signal in HEK293T cells, indicating that Gpr161 expression leads to $G\alpha_s$ stimulation. As a control, we used the canonical GPCR β2 adrenergic receptor (β2AR), which can be further stimulated by isoproterenol treatment (Fig. 4A). The PKA Rluc PCA assay measures the binary interaction between the catalytic (C) and regulatory (R) subunits of PKA, where reduced bioluminescence indicates the dissociation of PKA R from PKA C, and the activation of PKA. Expression of Gpr161 in IMCD3 cells resulted in decreased PKA PCA bioluminescence, indicating that Gpr161 activities trigger the dissociation of PKA holoenzyme complexes (Fig. 4B). Based on these data, we conclude that Gpr161 displays constitutive basal activities to activate $G_{\alpha s}$ and thus PKA. If the phenotypes observed in the *gpr161* mutants are due to a loss of adenylate cyclase (AC) activity, we would expect that the artificial activation of AC by general cAMP-elevating agents, such as forskolin, should rescue the mutant embryos. Previous studies have reported that 300 µM forskolin phenocopies a complete loss of Hh signalling (Barresi et al., 2000). Treatment with 300 µM forskolin resulted in a near-complete loss of all MPs and SSFs in wild-type as well as *gpr161* mutant embryos (Fig. 4C-E), whereas treatment with lower concentrations, ranging from 500 nM to 50 µM, which had only minor effects on somite development of wild-type embryos, resulted in a near-complete rescue of the number and organisation of SSFs and MPs in the *gpr161* mutants (Fig. 4C-E). These results are consistent with the model that derepression of Hh signalling in the *gpr161* mutants is due to a reduction of PKA activity.

### PKA regulates the activity and ciliary localisation of Gpr161

To further investigate the mechanism by which Gpr161 regulates vertebrate Hh signalling, we tested whether the *gpr161* mutant phenotype could be rescued by injection of tagged *Gpr161* mRNA. Injection of either mCherry-tagged mouse or Myc-tagged zebrafish *gpr161* mRNA resulted in a near-complete rescue of the morphological and molecular phenotypes of the *gpr161* mutant embryos (Fig. 5B,C, Fig. S8). In mammalian cell culture, overexpression of mGpr161 was shown to inhibit Hh signalling (Pusapati et al., 2018). In contrast, injection of even very high levels of mRNA (up to 400 pg) did not inhibit Hh signalling in zebrafish embryos, as assessed by morphology and molecular markers (Fig. 5A). Injection of mRNA encoding mGpr161$^{376\text{-S/T>A-401}}$, a mutant form that remains ciliary in the presence of activated Hh signalling (Pal et al., 2016), similarly had no effect on Hh target gene expression (Fig. 5A). Thus, in contrast to mammalian cell culture, overexpression of Gpr161 does not inhibit Hh signalling in zebrafish embryos. We next determined to what extent mutant forms of mGpr161 were able to rescue the zebrafish *gpr161* mutant phenotype. The degree of rescue was assessed by staining for Prox1 and Eng to facilitate quantification of Hh signalling at high resolution. mGpr161$^{V128E}$ carries a mutation that affects a putative G-protein-coupling domain of Gpr161 in the second intracellular loop (ICL2), and was shown to block the ability of Gpr161 to induce increased cAMP levels in mammalian cells (Mukhopadhyay et al., 2013). Surprisingly, injection of *mGpr161*$^{V128E}$ mRNA into *gpr161* mutant embryos resulted in a rescue of the mutant phenotype, similar to injection of wild-type *mGpr161* mRNA (Fig. 5B,C). A rescue was also observed with mRNA of the equivalent zebrafish mutant, Gpr161$^{V125E}$ (data not shown). These results suggest that, in zebrafish embryos, mGpr161$^{V128E}$ and zebrafish Gpr161$^{V125E}$ retain the ability to activate $G_{\alpha s}$.

We have previously shown that Gpr161 binds selectively to PKA type I regulatory subunits (R), and recruits RIα to primary cilia in zebrafish embryos, suggesting that Gpr161 acts as an A-kinase anchoring protein (Bachmann et al., 2016). To determine whether Gpr161 binds PKA holoenzymes, we used a NLuc-based BRET assay to measure the interaction between Gpr161-GFP10 and NLuc-RI-C (Fig. S9C), and found that Gpr161 recruits the RI-C holoenzyme through its AKAP domain (Fig. S9D). We conclude that Gpr161 acts as an AKAP to recruit PKA holoenzymes to the cilium. Although the presence of this AKAP domain within the intracellular domain of Gpr161 might indicate that Gpr161 plays a role in ensuring that PKA holoenzymes localise to the cilium to phosphorylate the Gli transcription factors, type I PKA typically acts on targets in very close proximity to the holoenzyme-AKAP complex (Diskar et al., 2007; Martin et al., 2007; Taylor et al., 2012). We have shown that Gpr161 contains a PKA consensus phosphorylation site, which is phosphorylated by PKA *in vitro* and *in vivo* (Bachmann et al., 2016), raising the possibility that Gpr161-dependent ciliary type I PKA may be involved in the regulation of Gpr161 itself. Both the AKAP domain and the PKA phosphorylation site are conserved in both zebrafish Gpr161 paralogues, and in homologues in other species (Fig. S1). To test this hypothesis, we attempted to rescue the zebrafish *gpr161* mutants with mRNAs encoding an AKAP-domain mutant (mGpr161$^{L465P}$), which abolishes RI binding to Gpr161, and a phosphorylation-deficient form of Gpr161, where the two consensus site serine residues have been mutated to alanines, mGpr161$^{S428A,\ S429A}$ (Bachmann et al., 2016). We found that although injection of either *mGpr161*$^{L465P}$ or *mGpr161*$^{S428A,S429A}$ mRNA significantly reduced the number of both SSFs and MPs, the SSFs were reduced to levels similar to those observed with wild-type mGpr161 rescue, whereas

Development (2021) 148, dev192443. doi:10.1242/dev.192443

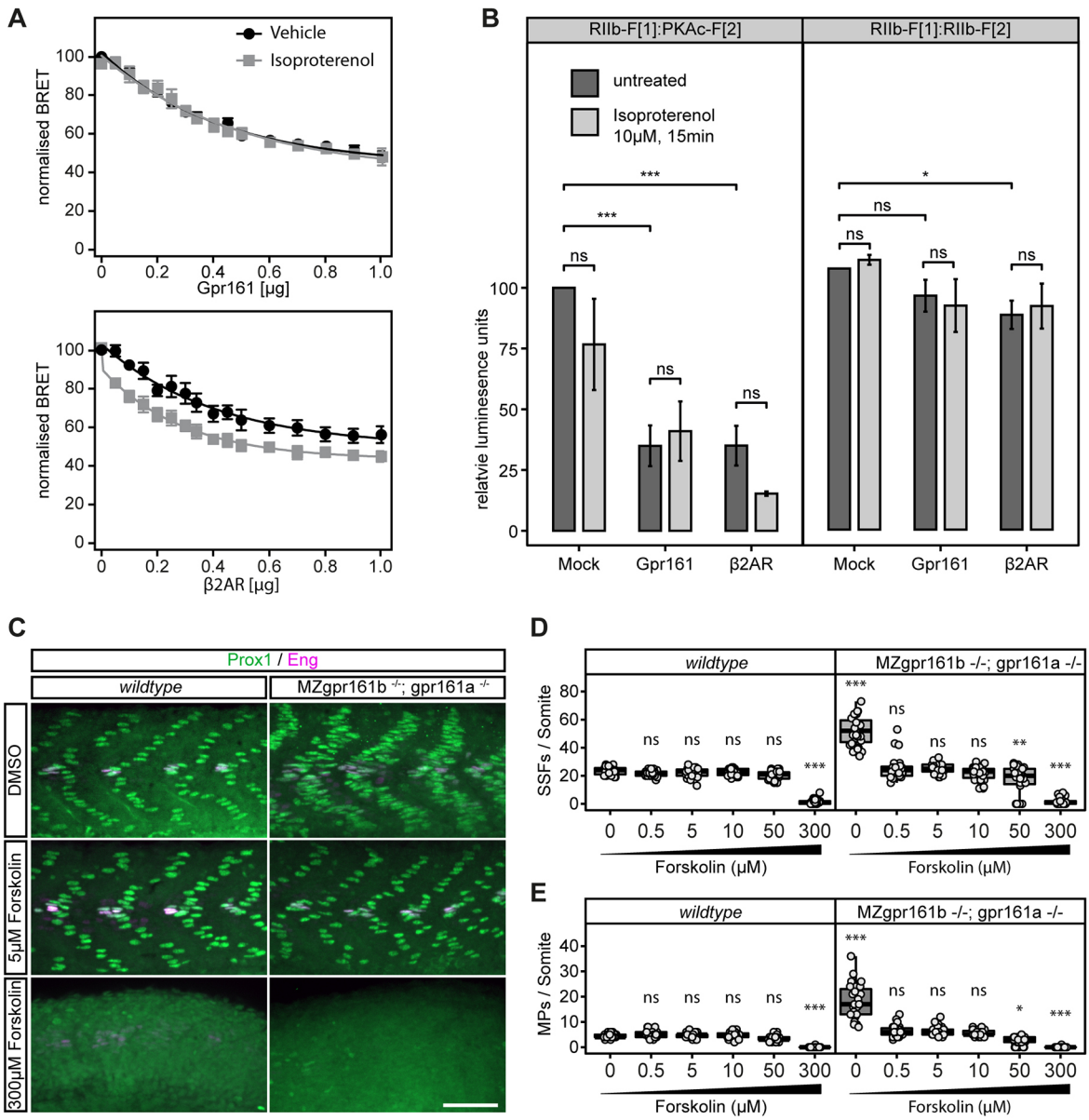


**Fig. 4. cAMP elevation rescues the gpr161 phenotype.** (A) The reporter constructs, together with increasing concentrations of β2AR (positive control) and Gpr161 receptor constructs, were transiently expressed in HEK293 cells followed by treatment with the β2AR-specific agonist isoproterenol (10 µM, 15 min). BRET readout was measured using the Mithras LB 940 plate reader (±s.d. of *n*=4 independent experiments), and normalised to the 0 µg receptor transfection experiments. (B) IMCD3 cells were transiently transfected with the constructs for the PKAc:RIIb RLuc PCA combination to assess PKA activation in response to Gpr161 and β2AR expression, and stimulation by isoproterenol (10 µM for 15 min). RIIb-F1/RIIb-F2 RLuc PCA constructs were used as a negative control. The readouts were normalised to untreated 0 µg receptor transfection experiments (±s.d. of *n*=3 independent experiments; ***$P$<0.001, *$P$<0.05; ns, not significant; two-way ANOVA, Tukey's post-hoc test for pairwise comparisons). (C) Prox1 (green)/Eng (purple) immunostaining of wild-type and MZ*gpr161b*$^{-/-}$; *gpr161a*$^{-/-}$ embryos treated with increasing concentrations of forskolin. Scale bar: 50 µm. (D,E) Quantification of SSFs and MPs in wild-type and MZ*gpr161b*$^{-/-}$; *gpr161a*$^{-/-}$ embryos treated with increasing concentrations of forskolin (for each experiment, *n*=27 somites in nine embryos; ***$P$<0.001, **$P$<0.01, *$P$<0.05; ns, not significant; two-way ANOVA, Tukey's post-hoc test for pairwise comparisons). Box plots show median values (centre lines) and the interquartile ranges (boxes); whiskers extend to the highest and lowest values within 1.5×IQR (inter-quartile range).

the number of MPs was significantly higher than embryos injected with wild-type *mGpr161* mRNA (Fig. 5B,C, Fig. S8). To investigate the relative numbers of SSFs and MPs, we plotted the ratios of SSFs to MPs in wild-type, mutant and rescued mutant embryos (Fig. 5D). Wild-type embryos have a mean SSF/MP ratio of 5.6, whereas in uninjected mutants this ratio is 2.4. Both mGpr161$^{V128E}$ and wild-type mGpr161 fully restored the ratio of SSFs/MPs, whereas ratios of SSFs/MPs in mutants injected with either *mGpr161*$^{L465P}$ or *mGpr161*$^{S428A,S429A}$ mRNA were not significantly different from those of uninjected mutants. These results suggest that phosphorylation of the PKA consensus site(s) of Gpr161, and the close proximity of the PKA holoenzyme to Gpr161, is required for its correct function in the regulation of Hh signalling. To determine whether these mutations alter the ability of Gpr161 to activate $G_{\alpha s}$ and PKA, we applied the $G_{\alpha s}$ NLucII-GFP10 BRET assay to test wild-type Gpr161, as well as Gpr161$^{L465P}$, Gpr161$^{S428A, S429A}$ and Gpr161$^{V128E}$ (Fig. S9). We found no significant difference between wild-type and mutant Gpr161 in either of these assays. These results suggest that phosphorylation of Gpr161 by PKA is not involved in regulating its ability to activate $G_{\alpha s}$, and additionally that

Development (2021) 148, dev192443. doi:10.1242/dev.192443

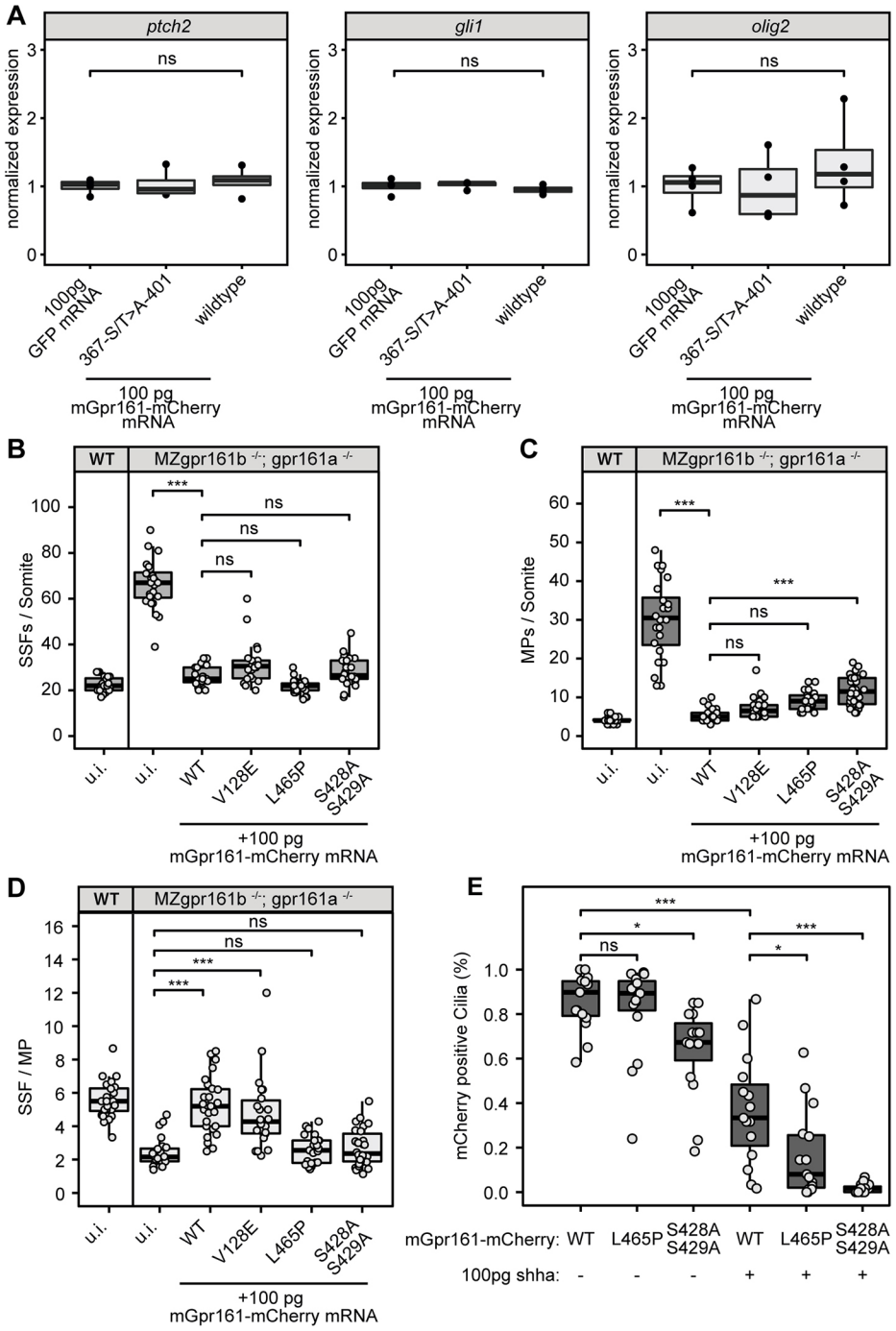


**Fig. 5. Overexpression of mGpr161-mCherry in wild-type and MZ*gpr161b*$^{-/-}$; *gpr161a*$^{-/-}$ embryos.** (A) Injections of 100 pg *mGpr161*$^{376\text{-}S/T>A\text{-}401}$*-mCherry* or wild-type *mGpr161-mCherry* mRNA do not lead to an upregulation of the Hh-targets *ptch2*, *gli1* or *olig2* compared with control injections with 100 pg GFP mRNA ($n$=4; ns not significant, Kruskal–Wallis rank sum test). (B,C) Quantification of SSFs and MPs upon injection of different mGpr161 mRNAs into *gpr161* mutants ($n$=22-27 somites in seven to nine embryos; ***$P$<0.001, *$P$<0.05; ns, not significant; one-way ANOVA, Tukey's post-hoc test for pairwise comparisons). Wild-type uninjected values are shown for comparison. (D) SSF/MP ratios within the somites quantified in B,C. (E) Quantification of mCherry-positive cilia at 9 hpf after injection of 100 pg mRNA of mGpr161-mCherry transcripts in response to co-injection of 100 pg *shha* mRNA ($n$=15 embryos from three experiments; ***$P$<0.001, *$P$<0.05; ns, not significant, two-way ANOVA, Tukey's post-hoc test for pairwise comparisons). Box plots show median values (centre lines) and the interquartile ranges (boxes); whiskers extend to the highest and lowest values within 1.5×IQR (inter-quartile range).

the V128E substitution is not sufficient to abolish G protein coupling and activation by Gpr161.

To determine whether phosphorylation of the PKA consensus site of Gpr161 regulates its subcellular localisation, we injected mCherry-tagged wild-type *mGpr161*, *mGpr161*$^{L465P}$ and *mGpr161*$^{S428A,S429A}$ mRNAs into wild-type embryos, and quantified the percentage of Gpr161-mCherry-positive cilia. All three forms of Gpr161 were readily detected at the cilium at 9 hpf (Fig. 5E, Fig. S10). Although the percentage of Gpr161-mCherry-positive cilia was relatively variable, we found no significant differences between wild-type mGpr161-mCherry and mGpr161$^{L465P}$-mCherry (Fig. 5E, Fig. S10). However, we observed a slight, but significant reduction in the percentage of mGpr161$^{S428A,S429A}$-mCherry-positive cilia (Fig. 5E, Fig. S10). Co-injection of *shh* mRNA significantly reduced the percentage of cilia positive for wild-type Gpr161-mCherry, consistent with previous reports (Mukhopadhyay et al., 2013; Pusapati et al., 2018), although it did not abolish the ciliary localisation of Gpr161-mCherry. However, in the presence of Shh, Gpr161$^{L465P}$-mCherry showed a much stronger reduction of ciliary localisation, whereas little or no Gpr161$^{S428A,S429A}$-mCherry was detected on the cilium. Taken together, these results suggest that the phosphorylation of Gpr161 by PKA may regulate the dynamics of ciliary localisation of Gpr161.

## DISCUSSION

Hh signalling is tightly controlled at multiple levels in order to accurately translate morphogen gradients into graded transcriptional

Development (2021) 148, dev192443. doi:10.1242/dev.192443

responses mediated by the Gli transcription factors. PKA both promotes formation of the Gli repressor forms and inhibits Gli activator forms, thereby controlling sensitivity to Hh ligands, and providing a filter for Hh signalling strength. How PKA activity is fine-tuned in Hh signalling is not completely understood. GPCRs such as Gpr161 have been shown to impact Hh signalling by regulating PKA via the regulation of adenylate cyclase activity. To extend our understanding of how GPCRs regulate Hh signalling, we generated zebrafish *gpr161* mutants and analysed Hh-dependent signalling in the neural tube and the myotome.

The zebrafish genome contains two conserved Gpr161 orthologues, Gpr161a and Gpr161b. We have generated mutants for both paralogues, and show that Gpr161a and Gpr161b act redundantly in early zebrafish development. Zebrafish mutants lacking Gpr161 function show an expansion of Hh target gene expression both in the neural tube and in the somites, and develop severe craniofacial defects that are similar to, although less severe than, those described for the *ptc1*$^{-/-}$*; ptc2*$^{-/-}$ double mutants (Koudijs et al., 2005, 2008). Similarly, injection of a dominant-negative form of PKA resulted in a stronger increase of Hh-dependent muscle cell specification in the myotome compared with what we observed in *gpr161* mutants (Zhao et al., 2016). This is consistent with data obtained in mice, where a loss of PKA or $G_{\alpha s}$ leads to more severe ventralisation of the neural tube than that observed in the *gpr161* mutants (Mukhopadhyay et al., 2013; Pusapati et al., 2018; Regard et al., 2013; Tuson et al., 2011). Further supporting the idea that Hh signalling is not maximally activated in the *gpr161* mutants, we find that injection of *shha* mRNA can further increase high-, but not low-level Hh targets in the somites of *gpr161* mutants. Thus, we conclude that, whereas low-level Hh signalling is maximally active in the *gpr161* mutants, additional mechanisms contribute to PKA activation to control high-level Hh signalling in the absence of Gpr161 function.

We also show that low-level Hh signalling in the neural tube of *gpr161* mutants is independent of Smo, whereas expression of the high-level Hh target gene *nkx2.2a* clearly requires Smo function. Our results are consistent with the model that $G_{\alpha s}$-coupling and activation by Gpr161 is one of several mechanisms that contribute to the mobilisation of cAMP to repress Hh target activation, and that the reduction in cAMP levels caused by loss of Gpr161 is sufficient to cause Smo-independent activation of low, but not maximal, levels of Hh signalling. This result provides genetic evidence to support the model based on results from pharmacological inhibition of Smo in mammalian cell culture (Pusapati et al., 2018). Similar experiments performed in mouse *Gpr161* mutants showed that Gpr161 is largely epistatic to Smo (Mukhopadhyay et al., 2013). These authors do, however, note that the expression of high-level Hh target genes, such as *Nkx2.2* and *Foxa2*, is reduced in *Smo; Gpr161* double mutants compared with *Gpr161* single mutants. This difference may be due to the different assays used to assess Hh target gene expression in mouse and zebrafish neural tubes. Whereas Mukhopadhyay and colleagues used immunohistochemistry to detect Hh target expression (Mukhopadhyay et al., 2013), our results are based on chromogenic *in situ* hybridisation, a far less sensitive assay. Thus, we cannot rule out that some low-level *nkx2.2a* expression persists in the zebrafish triple mutants. Another possibility is that there are species-specific differences in the roles of GliR and GliA and/or cAMP levels, or, alternatively, Gpr161 might make a relatively larger contribution to cAMP levels in the zebrafish neural tube compared with mouse. These results confirm that the role of Gpr161 as a modulator of Hh signalling is conserved in the vertebrate lineage.

Gpr161 has been proposed to contribute to the basal Hh repression machinery by activating $G_{\alpha s}$, and overexpression of murine Gpr161 has been shown to lead to a general increase in intracellular cAMP levels (Mukhopadhyay et al., 2013). However, direct evidence for reduced cAMP production in *Gpr161* mutant cells is hampered by the difficulties in measuring physiological cAMP levels in specific subcellular compartments such as the primary cilium. We have taken advantage of the amenability of the zebrafish embryo to pharmacological and embryological manipulation to further probe the mechanism of Gpr161 action. Consistent with the model that loss of Gpr161 leads to lowered cAMP levels and reduced PKA activity, we found that treatment with the cAMP elevating agent forskolin fully rescued muscle cell specification in the *gpr161* mutant embryos. Interestingly, a 100-fold concentration range (0.5-50 µM) of forskolin gave very similar near-complete rescue of both mutant morphology and molecular read-outs of both high- and low-level Hh target gene expression in the somites, suggesting that additional mechanisms may be in place to ensure appropriate regulation of PKA activity in the presence of excess cAMP. Previous studies have reported that loss of Gpr161 may also affect other signalling pathways in addition to Hh signalling (Li et al., 2015; Mukhopadhyay et al., 2013). Although we cannot rule out a role for Gpr161 in processes not related to Hh signalling, our results suggest that loss of Gpr161 function can be fully compensated for by artificial activation of adenylate cyclase.

However, an artificial increase in cAMP levels would be expected to rescue any Hh gain-of-function phenotype that results from dysregulation of Hh signalling upstream of the Gli transcription factors. A more-direct test of Gpr161 acting as a $G_{\alpha s}$-coupled receptor in regulating Hh signalling is to determine whether a $G_{\alpha s}$-coupling-deficient mutant can restore regulation of Hh signalling in the zebrafish *gpr161* mutants. We found that injection of mGpr161$^{V128E}$, a mutant that was previously shown to abolish the increase in cAMP levels seen with wild-type mGpr161, resulted in a rescue of the mutant phenotypes comparable with that seen with injection of wild-type mGpr161 (Fig. 5B,C). One caveat in interpreting this result is that a definitive GPCR G-protein-binding domain has been notoriously difficult to identify, with residues in ICL1-ICL3 and also TM domains contributing to G-protein binding and activation (Oldham and Hamm, 2008). Consistent with this, we found that the V128E does not abolish $G_{\alpha s}$ and PKA activation by mGpr161.

Previous studies have shown that in the absence of Hh, Gpr161 localises to cilia, and that activation of Hh signalling, involving the ciliary translocation of active Smo and activation of Grk2, induces the ciliary exit of Gpr161 (Mukhopadhyay et al., 2013; Pal et al., 2016). This inverse correlation suggests a simple model where the ciliary Gpr161 receptor and AKAP functions contribute to the maintenance of high cAMP levels and PKA activity in the cilium; the inhibition of PKA activity within the cilium, which allows activation of the Gli transcription factors, is achieved by the ciliary exit of Gpr161. However, this model has been questioned, as some observations suggest that the ciliary localisation of Gpr161 does not strictly correlate with its ability to antagonise Hh signalling (Pusapati et al., 2018). Notably, mGpr161$^{vl}$, a C-terminus truncation mutant, remains on the cilium even in the presence of activated Smo, but does not inhibit Hh signalling (Li et al., 2015; Matteson et al., 2008; Pal et al., 2016). Consistent with this, we found that overexpression of mGpr161$^{376\text{-}S/T>A\text{-}401}$, which remains in the cilium upon Smo activation (Pal et al., 2016), did not inhibit Hh signalling in zebrafish embryos. However, Gpr161$^{vl}$ has been shown to recruit high levels of β-arrestin (Pal et al., 2016), raising the possibility that ciliary Gpr161$^{vl}$ may be non-functional. Supporting this, *Gpr161*$^{vl}$ mutant embryos show a moderate increase in Hh target genes such as *Ptch1* and *Gli1* (Li et al., 2015).

Development (2021) 148, dev192443. doi:10.1242/dev.192443

Other observations support the idea that the ability of Gpr161 to antagonise Hh signalling depends on its ciliary localisation. Our results suggest that PKA plays a role in regulating Gpr161, and that Gpr161 may act as an AKAP to ensure efficient phosphorylation of Gpr161 itself. Injection of the AKAP-deficient form mGpr161$^{L465P}$ or the PKA phosphorylation-deficient mGpr161$^{S428A,S429A}$ largely rescued the morphological phenotype of *gpr161* zebrafish mutants, although molecular analysis showed that, whereas SSFs were reduced to near wild-type levels, injected mutant embryos still possessed supernumerary MPs. One possibility is that the loss of PKA phosphorylation allows the rescue of low, but not high, levels of Hh signalling. However, a preferential rescue of low compared with high-level Hh signalling appears difficult to reconcile with the widely accepted direct role for Gpr161 in activating PKA. An alternative model is that mGpr161$^{S428A,S429A}$ (and mGpr161$^{L465P}$) is fully functional and does in fact restore cAMP levels in the *gpr161* mutants, but that the downregulation of Gpr161 activity is affected by the S428A,S429A mutation. Such a hypothesis is supported by our observations that wild-type mGpr161 and mGpr161$^{S428A,S429A}$ activate $G_{\alpha s}$ equally well, and that mGpr161$^{S428A,S429A}$ show reduced ciliary localisation compared with wild-type mGpr161 (Fig. 5E, Fig. S9E).

The ciliary localisation of GPCRs is dynamic, and depends on the active transport into and out of the cilium. In addition, recycling through distinct endocytotic pathways will influence the level of any given GPCR within the cilium. The Hh-dependent ciliary export of Gpr161 has been shown to be reversible (Pal et al., 2016). We show here that, in randomly selected cells of the late gastrula stage zebrafish embryo, the ciliary localisation of mGpr161$^{S428A,S429A}$ is reduced compared with wild-type mGpr161 (wild type 86±13% versus mutant 64±20%, mean±s.d.). However, in a defined region close to the dorsal midline, we previously found no significant difference in ciliary localisation between wild-type mGpr161-mCherry and mGpr161$^{S428A,S429A}$ (wild type 74±12% versus mutant 72±13%, mean±s.d.; Bachmann et al., 2016), suggesting that, in cells exposed to medium-to-high levels of Hh ligand, mGpr161$^{S428A,S429A}$ behaves in a similar manner to wild-type mGpr161, and that a significant difference between wild-type and mutant mGpr161 is observed only when cells that are exposed to little or no endogenous Hh ligand are included, as is the case in our present analysis (Fig. 5E, Fig. S10). The Hh-induced ciliary export of Gpr161 has been shown to depend on Grk2 phosphorylation of, and β-arrestin recruitment to, S/T residues in the C-terminal tail (Pal et al., 2016). Importantly, the Grk2 phosphorylation site (residues 376-401) is distinct from, though adjacent to the PKA phosphorylation site (residues 428-429; Bachmann et al., 2016), and these phosphorylation events have opposite effects on ciliary localisation. One possibility is that PKA phosphorylation might counteract or limit phosphorylation by Grk2. Alternatively, PKA phosphorylation might target Gpr161 for specific rapid recycling of Gpr161 to the cilium. Both of these scenarios are consistent with the near-complete loss of ciliary mGpr161$^{S428A,S429A}$ upon Shh mRNA injection (Fig. 5E).

We propose that the phosphorylation of Gpr161 by PKA may constitute a feedback mechanism to allow the fine-tuning of Gpr161-dependent PKA activity in response to Shh. In the absence of Hh, high PKA activity could phosphorylate Gpr161 to promote a slow export, or rapid recycling, of ciliary Gpr161, which would contribute to the maintenance of high PKA activity. In the presence of high levels of Hh, decreased PKA activity (and Gpr161 phosphorylation) would promote the rapid exit or reduced recycling of Gpr161 to ensure that PKA activity levels remain low for a sufficient period of time to promote high-level Hh signalling outcomes. Although we cannot rule out the possibility that Gpr161 may function also outside the cilium, our results suggest that the ability of Gpr161 to antagonise Hh signalling depends on its ciliary localisation, and that phosphorylation of Gpr161 by PKA regulates its ability to modulate Hh signalling outcomes.

## MATERIALS AND METHODS

### CRISPR/cas9 genome editing and genotyping

Guide RNAs for CRISPR/cas9 mediated knockout of both *gpr161a* (ENSDART00000151311.2) and *gpr161b* (ENSDART00000078051.6) were designed using the ChopChop web tool (Montague et al., 2014) and synthesised as described previously (Huang et al., 2014). Embryos were injected with 50 pg of gene-specific sgRNA and 300 pg of *cas9* mRNA at 1-cell stage. F0 founder fish were identified by T7 Endonuclease I digests of gene-specific PCR products from pooled genomic DNA obtained from F1 offspring, following the manufacturer's protocol (NEB, #M0302L). Although the *gpr161a*$^{ml200}$ allele harbours an 8 bp deletion, the introduced mutation in *gpr161*$^{ml201}$ leads to a 6 bp insertion, which were identified by running out gene-specific PCR products (see Table S2) on 4% agarose gels. Genotyping of the *smo*$^{hi1640}$ allele was performed as described previously (Chung and Stainier, 2008).

### Zebrafish lines and husbandry

All zebrafish lines, including SAT wild-type strains, were kept at 28°C according to standard protocols. MZ*gpr161b*$^{-/-}$; *gpr161a*$^{-/-}$ embryos were obtained by performing in-crosses of a *gpr161b*$^{-/-}$; *gpr161a* $^{+/-}$ line. Embryos were raised at 28°C and staged by morphology (Kimmel et al., 1995).

All experimental protocols concerning zebrafish were approved by the Austrian Ministry for Science and Research (BMWFW-66.008/0016-WF/V/3b/2016 and BMBWF-66.008/0015-V/3b/2018), and experiments were carried out in accordance with approved guidelines.

### Construction of plasmids

To generate expression vectors for *gpr161a* and *gpr161b*, both coding sequences were amplified with overlapping primers (see Table S2) using homemade PfuX7 polymerase (Nørholm, 2010) and fused in-frame to a Myc-tag into pCS2+ by *in vivo* Assembly (IVA) cloning (García-Nafría et al., 2016). pcDNA3.1 mGpr161-mCherry constructs (wild type, L465P and S428A/S429A) have been described previously (Bachmann et al., 2016). mGpr161$^{376\text{-}S/T>A\text{-}401}$ (Pal et al., 2016) was introduced into the same expression vector by restriction cloning. mGpr161$^{V128E}$, which was originally described as mGpr161$^{V158E}$ due to the use of a slightly longer isoform of mGpr161 (Mukhopadhyay et al., 2013), was created by site-directed mutagenesis (see Table S2 for primer sequences) of wild-type mGpr161-mCherry following standard protocols. All expression constructs were verified by sequencing of the respective open reading frame.

### Quantitative (q) RT-PCR

RNA was isolated from zebrafish embryos with Trizol (Ambion) following the manufacturer's instructions. RNA integrity was checked by agarose gel electrophoresis and the concentration was measured using a Nanodrop 2000c (Thermo) spectrophotometer. Complementary DNA was transcribed from equal amounts of dsDNase-treated total RNA using the Maxima RT kit for qPCR (Thermo) with dsDNase according to the manufacturer's instructions.

RT-qPCRs were performed using 5× HOT FIREPol EvaGreen qPCR Supermix (Solis Biodyne) and contained each primer at 250 nM and cDNA corresponding to a total RNA amount of 15 ng for pooled embryos or 5 ng for single embryos. PCRs were run on a CFX96 Connect (Bio-Rad) under the following conditions: 12 min at 95°C, 40 cycles of 95°C for 30 s, 60°C for 30 s and 72°C for 20 s. Melt curves were recorded from 65°C to 95°C in 0.5°C increments. Data were acquired using CFX Manager 3.1 (Bio-Rad) and exported as RDML files for processing.

Data analysis was performed in R version 3.4.4. Fluorescence data were imported using the package RDML (Rödiger et al., 2017) and amplification curves fitted using the 'cm3' model (Carr and Moore, 2012) implemented in the package qpcR (Ritz and Spiess, 2008). The first derivative (d0) of the

Development (2021) 148, dev192443. doi:10.1242/dev.192443

model was used as expression value. Expression values for genes of interest were normalised using the geometric mean of the expression values of the reference genes *eef1aa* and *rpl13*.

### Whole-mount *in situ* hybridisation

*In situ* hybridisation was performed following standard protocols. DIG-labelled antisense probes were made for *shha* (Krauss et al., 1993), *ptch2* (Concordet et al., 1996), *olig2* (Park et al., 2002), *nkx2.2a* (Barth and Wilson, 1995) and *cmlc2* (Yelon et al., 1999).

### Immunohistochemistry

Embryos were fixed in 4% paraformaldehyde at room temperature for 3 h, then washed in PBS-Triton (PBS+0.3% Triton X-100). After 1 h of incubation in blocking solution (PBS-Triton, 4% BSA, 0.02% $NaN_3$) at 4°C, primary antibodies diluted in blocking solution were added and left overnight for incubation at 4°C. After subsequent washes in PBS-Triton, embryos were incubated with appropriate Alexa-conjugated secondary antibodies overnight at 4°C. Again, embryos were washed several times in PBS-Triton and mounted in Mowiol embedding medium for imaging. For a list of the antibodies used in this study, see Table S1.

Ciliary localisation of Gr161 as presented in Fig. 1 was imaged using a Zeiss Axio Observer.Z1 microscope equipped with a Yokogawa CSU-X1 spinning disc confocal unit using a Zeiss C-Apochromat 63×/1.20 W Korr UV VIS IR lens.

Prox1/Engrailed stainings were imaged using a Zeiss Axio Observer.Z1 microscope equipped with a Yokogawa CSU-X1 spinning disc confocal unit using a Zeiss LD LCI Plan-Apochromat 25×/0.8 Imm autocorr DIC lens, or a Zeiss LSM 700 Axio Imager using a Zeiss Plan-Apochromat 63×/1.40 Oil DIC lens. The images presented in Fig. S10 were taken on a Leica DMi8 using a Leica HC PL APO 63×/1.40 Oil lens. For the quantification of MPs and SSFs, Prox1/Eng double-positive nuclei (SSFs) and nuclei that were only positive for Prox1 (SSFs) were counted manually by going through the 3D image stack. Nuclei that were only positive for Eng (medial fast fibres, see Wolff et al., 2003) were not included in the analysis. For each embryo, three somites were selected at the same A-P position of the embryo across all experiments, using the yolk extension of the zebrafish embryos as a reference point.

### Chemical treatments

For chemical treatments, embryos were dechorionated at 50% epiboly and transferred to agar-coated 35 mm dishes containing either: forskolin (Biomol) at final concentrations between 0.5 and 300 µM in egg water containing 1% DMSO; or cyclopamine (Biomol) at final concentrations between 5 and 15 µM in egg water containing 1% DMSO. Control experiments were performed simultaneously in egg water containing 1% DMSO. All embryos were treated until 24 hpf.

### Microinjection

mRNA was synthesised using the HiScribe SP6 RNA Synthesis Kit (NEB) and capped using the Vaccinia Capping System (NEB) following the protocols provided by the manufacturer. Embryos were injected at one-cell stage. Injected amounts of mRNA are indicated in the respective figures.

### Light histology

Three-day-old (72 hpf) wild-type and *gpr161* mutant embryos were fixed in 2.5% glutaraldehyde in 0.01 M sodium cacodylate buffer for 2 h, washed in buffer, dehydrated in an increasing acetone series and embedded in EMBed 812 epoxy resin. After polymerisation for 48 h at 60°C, embryos were cut serially with an Autocut 5020 (Reichert) and a Diatome Butler knife. Serial sections (2 µm) were stained according to Richardson et al. (1960) for 10 min, washed and mounted in cedarwood oil. Images were taken with a Leica DM5000B microscope using a Leica DFC 490 digital camera and Leica application suite v. 4.8.

### Electron microscopy

Embryos were fixed with 2.5% glutaraldehyde in 0.01 M sodium cacodylate buffer containing 5% sucrose at 4°C for 2 h. After washing in cacodylate buffer, specimens were post-fixed in reduced osmium (2% osmium tetroxide and 3% potassium ferrocyanide in 0.1 M cacodylate buffer) for 2 h at 4°C, dehydrated in an ethanol series, critical point dried with an EMS 850 CPD, mounted and 20 nm gold sputtered with a CCU-010 sputter coater (Safematic, Switzerland), and examined with a DSM950 scanning electron microscope (Zeiss, Germany). Images were taken with a Pentax digital camera and PK_Tether 0.7.0 free software.

### BRET measurements

HEK293 cells were detached with trypsin and seeded at a concentration of 350,000 cells/ml. Next, the DNA was transfected using linear polyethylenimine (PEI, 516 Polysciences) with a DNA:PEI ratio of 1:3. For the Gpr161-Gαs coupling experiments, the three-component BRET-based biosensor Gαβγ, consisting of, pcDNA3-Gαs67-RlucII (25 ng), pcDNA3-Gβ1 (50 ng) and pcDNA3-Gγ1-GFP10 (75 ng) (Galés et al., 2005) was used for transfection in a 1:2:3 ratio together with increasing concentrations of pcDNA-β2AR or wild-type and mutant pcDNA-Gpr161 constructs (0-1 µg). For the PCA-BRET biosensor experiments, the two-component PCA-based biosensor (300 ng of pcDNA3-RIIb-NLucF1 and 300 ng pcDNA3-C-NLucF2) and the pcDNA3-Gpr161-YFP construct (600 ng) were used. Directly after transfection, cells were plated in white 96-well culture plates at a concentration of 35,000 cells per well and were incubated at 37°C. Forty-eight hours after transfection, cells were washed with stimulation buffer (Thyrode HEPES 519 buffer, THB) and incubated for 1 h at 37°C. The luciferase substrate DeepBlueC (DBC) was added 5 min before BRET reading. BRET was monitored with a Mithras LB 940 microplate reader (Berthold Technologies) equipped with a donor filter of 410/80 nm and an acceptor filter of 515/40 nm (=BRET2). For PCA BRET biosensor measurements, a donor filter of 485/20 nm and an acceptor filter of 530/25 nm (=BRET1) was used. In all cases, the BRET ratio was calculated by dividing the acceptor emission over the donor emission.

### PCA measurements

IMCD3 cells were seeded into 24-well culture plates 1 day before transfection. Transient transfection using equal amounts (0.1 µg) of each of the RLuc-PCA biosensor components (pcDNA3-RIIb-F2+pcDNA3-C-F1 and pcDNA3-RIIb-F1+pcDNA3-RIIb-F2) and the respective GPCR (pcDNA3-β2AR and pcDNA3-Gpr161) was performed using TransFectin (Bio-Rad) as a transfecting agent. 48 h post-transfection the cells were treated with isoproterenol (10 µM) for 15 min. Prior to measurement the cells were suspended in PBS and transferred to 96-well cell culture plates. Following addition of the RLuc substrate benzylcoelenterazine (5 µM; Nanolight) the RLuc bioluminescence signals were integrated for 10 s. Bioluminescence measurements were performed by using LMaxTMII384 luminometer (Molecular Devices) as previously described (Röck et al., 2019).

### Data presentation and analysis

All data presented in this study were analysed with R using the RStudio integrated development environment and plotted using the 'ggplot2' package (Rstudio Team, 2016; Wickham, 2016), with the exception of the plots in Fig. 4A and Fig. S9E, which were plotted using Graphpad Prism software.

A Kruskal–Wallis rank sum test was conducted to examine differences on the expression of genes within the different genotypes, pairwise comparisons were performed using Dunn's test and obtained *P* values were corrected for multiple comparisons using the Benjamini Hochberg method.

Statistical significance of differences in the number of MPs and SSFs, or in Gpr161-positive cilia between groups was determined using ANOVA and Tukey's post-hoc test for pairwise comparisons (*$P$<0.05; **$P$<0.01; ***$P$<0.001; ns not significant). Sample sizes ($n$) and additional details are given in the respective figure legends.

#### Acknowledgements

We are grateful to Dzenana Tufegdzic for fish care, to Saikat Mukhopadhyay for providing constructs, and to Robin Kimmel and Kathi Klee for helpful discussions and/or comments on the manuscript.

#### Competing interests

The authors declare no competing or financial interests.

### Author contributions

Conceptualization: P.M.T., P.A.; Methodology: P.M.T., D.R., E.S., P.A.; Validation: P.M.T., P.A.; Formal analysis: P.M.T., D.R., R.R.; Investigation: P.M.T., D.R., R.R., W.S., P.A.; Resources: D.M., M.B., S.G., E.S.; Data curation: P.M.T., W.S.; Writing - original draft: P.M.T., P.A.; Writing - review & editing: P.M.T., P.A.; Visualization: P.M.T.; Supervision: D.M., M.B., S.G., E.S., P.A.; Project administration: P.A.; Funding acquisition: E.S., P.A.

### Funding

This work was supported by funding from the Austrian Science Fund (FWF) and the Tyrolean Science Fund (TWF) (FWF P27338 to P.A., FWF P30441 and P32960 to E.S., and TWF 236277 to D.R.).

### Supplementary information

Supplementary information available online at
https://dev.biologists.org/lookup/doi/10.1242/dev.192443.supplemental

### References

**Ayers, K. L. and Thérond, P. P.** (2010). Evaluating smoothened as a G-protein-coupled receptor for Hedgehog signalling. *Trends Cell Biol.* **20**, 287-298. doi:10.1016/j.tcb.2010.02.002

**Bachmann, V. A., Mayrhofer, J. E., Ilouz, R., Tschaikner, P., Raffeiner, P., Röck, R., Courcelles, M., Apelt, F., Lu, T.-W., Baillie, G. S. et al.** (2016). Gpr161 anchoring of PKA consolidates GPCR and cAMP signaling. *Proc. Natl. Acad. Sci. USA* **113**, 7786-7791. doi:10.1073/pnas.1608061113

**Barresi, M. J., Stickney, H. L. and Devoto, S. H.** (2000). The zebrafish slow-muscle-omitted gene product is required for Hedgehog signal transduction and the development of slow muscle identity. *Development* **127**, 2189-2199.

**Barth, K. A. and Wilson, S. W.** (1995). Expression of zebrafish nk2.2 is influenced by sonic Hedgehog/vertebrate Hedgehog-1 and demarcates a zone of neuronal differentiation in the embryonic forebrain. *Development* **121**, 1755-1768.

**Briscoe, J. and Thérond, P. P.** (2013). The mechanisms of Hedgehog signalling and its roles in development and disease. *Nat. Rev. Mol. Cell Biol.* **14**, 416-429. doi:10.1038/nrm3598

**Briscoe, J., Sussel, L., Serup, P., Hartigan-O'Connor, D., Jessell, T. M., Rubenstein, J. L. R. and Ericson, J.** (1999). Homeobox gene Nkx2.2 and specification of neuronal identity by graded sonic Hedgehog signalling. *Nature* **398**, 622-627. doi:10.1038/19315

**Carr, A. C. and Moore, S. D.** (2012). Robust quantification of polymerase chain reactions using global fitting. *PLoS ONE* **7**, e37640. doi:10.1371/journal.pone.0037640

**Chen, W., Burgess, S. and Hopkins, N.** (2001). Analysis of the zebrafish smoothened mutant reveals conserved and divergent functions of Hedgehog activity. *Development* **128**, 2385-2396.

**Chung, W.-S. and Stainier, D. Y. R.** (2008). Intra-endodermal interactions are required for pancreatic β cell induction. *Dev. Cell* **14**, 582-593. doi:10.1016/j.devcel.2008.02.012

**Concordet, J. P., Lewis, K. E., Moore, J. W., Goodrich, L. V., Johnson, R. L., Scott, M. P. and Ingham, P. W.** (1996). Spatial regulation of a zebrafish patched homologue reflects the roles of sonic Hedgehog and protein kinase A in neural tube and somite patterning. *Development* **122**, 2835-2846.

**Corbit, K. C., Aanstad, P., Singla, V., Norman, A. R., Stainier, D. Y. R. and Reiter, J. F.** (2005). Vertebrate smoothened functions at the primary cilium. *Nature* **437**, 1018-1021. doi:10.1038/nature04117

**Dessaud, E., Yang, L. L., Hill, K., Cox, B., Ulloa, F., Ribeiro, A., Mynett, A., Novitch, B. G. and Briscoe, J.** (2007). Interpretation of the sonic Hedgehog morphogen gradient by a temporal adaptation mechanism. *Nature* **450**, 717-720. doi:10.1038/nature06347

**Diskar, M., Zenn, H.-M., Kaupisch, A., Prinz, A. and Herberg, F. W.** (2007). Molecular basis for isoform-specific autoregulation of protein kinase A. *Cell. Signal.* **19**, 2024-2034. doi:10.1016/j.cellsig.2007.05.012

**Galés, C., Rebois, R. V., Hogue, M., Trieu, P., Breit, A., Hébert, T. E. and Bouvier, M.** (2005). Real-time monitoring of receptor and G-protein interactions in living cells. *Nat. Methods* **2**, 177-184. doi:10.1038/nmeth743

**García-Nafría, J., Watson, J. F. and Greger, I. H.** (2016). IVA cloning: a single-tube universal cloning system exploiting bacterial in vivo assembly. *Sci. Rep.* **6**, 27459. doi:10.1038/srep27459

**Guner, B. and Karlstrom, R. O.** (2007). Cloning of zebrafish nkx6.2 and a comprehensive analysis of the conserved transcriptional response to Hedgehog/Gli signaling in the zebrafish neural tube. *Gene Expr. Patterns* **7**, 596-605. doi:10.1016/j.modgep.2007.01.002

**Hammerschmidt, M., Bitgood, M. J. and McMahon, A. P.** (1996). Protein kinase A is a common negative regulator of Hedgehog signaling in the vertebrate embryo. *Genes Dev.* **10**, 647-658. doi:10.1101/gad.10.6.647

**Gagnon, J. A., Valen, E., Thyme, S. B., Huang, P., Ahkmetova, L., Pauli, A., Montague, T. G., Zimmerman, S., Richter, C. and Schier, A. F.** (2014). Efficient mutagenesis by Cas9 protein-mediated oligonucleotide insertion and large-scale assessment of single-guide RNAs. *PLoS ONE* **9**, e98186. doi:10.1371/journal.pone.0098186

**Hui, C.-C. and Angers, S.** (2011). Gli proteins in development and disease. *Annu. Rev. Cell Dev. Biol.* **27**, 513-537. doi:10.1146/annurev-cellbio-092910-154048

**Humke, E. W., Dorn, K. V., Milenkovic, L., Scott, M. P. and Rohatgi, R.** (2010). The output of Hedgehog signaling is controlled by the dynamic association between suppressor of fused and the Gli proteins. *Genes Dev.* **24**, 670-682. doi:10.1101/gad.1902910

**Hwang, S.-H., White, K. A., Somatilaka, B. N., Shelton, J. M., Richardson, J. A. and Mukhopadhyay, S.** (2018). The G protein-coupled receptor Gpr161 regulates forelimb formation, limb patterning and skeletal morphogenesis in a primary cilium-dependent manner. *Development* **145**, dev154054. doi:10.1242/dev.154054

**Ingham, P. W., Nakano, Y. and Seger, C.** (2011). Mechanisms and functions of Hedgehog signalling across the metazoa. *Nat. Rev. Genet.* **12**, 393-406. doi:10.1038/nrg2984

**Jiang, J. and Hui, C.-C.** (2008). Hedgehog signaling in development and cancer. *Dev. Cell* **15**, 801-812. doi:10.1016/j.devcel.2008.11.010

**Kimmel, C. B., Ballard, W. W., Kimmel, S. R., Ullmann, B. and Schilling, T. F.** (1995). Stages of embryonic development of the zebrafish. *Dev. Dyn.* **203**, 253-310. doi:10.1002/aja.1002030302

**Klein, R. S., Rubin, J. B., Gibson, H. D., DeHaan, E. N., Alvarez-Hernandez, X., Segal, R. A. and Luster, A. D.** (2001). SDF-1 alpha induces chemotaxis and enhances sonic Hedgehog-induced proliferation of cerebellar granule cells. *Development* **128**, 1971-1981.

**Kok, F. O., Shin, M., Ni, C.-W., Gupta, A., Grosse, A. S., van Impel, A., Kirchmaier, B. C., Peterson-Maduro, J., Kourkoulis, G., Male, I. et al.** (2015). Reverse genetic screening reveals poor correlation between morpholino-induced and mutant phenotypes in Zebrafish. *Dev. Cell* **32**, 97-108. doi:10.1016/j.devcel.2014.11.018

**Koudijs, M. J., den Broeder, M. J., Keijser, A., Wienholds, E., Houwing, S., van Rooijen, E. M. H. C., Geisler, R. and van Eeden, F. J. M.** (2005). The Zebrafish mutants dre, uki, and lep encode negative regulators of the Hedgehog signaling pathway. *PLoS Genet.* **1**, e19. doi:10.1371/journal.pgen.0010019

**Koudijs, M. J., den Broeder, M. J., Groot, E. and van Eeden, F. J. M.** (2008). Genetic analysis of the two zebrafish patched homologues identifies novel roles for the Hedgehog signaling pathway. *BMC Dev. Biol.* **8**, 15. doi:10.1186/1471-213X-8-15

**Krauss, S., Concordet, J.-P. and Ingham, P. W.** (1993). A functionally conserved homolog of the *Drosophila* segment polarity gene hh is expressed in tissues with polarizing activity in zebrafish embryos. *Cell* **75**, 1431-1444. doi:10.1016/0092-8674(93)90628-4

**Lai, J. K. H., Gagalova, K. K., Kuenne, C., El-Brolosy, M. A. and Stainier, D. Y. R.** (2019). Induction of interferon-stimulated genes and cellular stress pathways by morpholinos in zebrafish. *Dev. Biol.* **454**, 21-28. doi:10.1016/j.ydbio.2019.06.008

**Leung, T. C., Humbert, J. E., Stauffer, A. M., Giger, K. E., Chen, H., Tsai, H.-J., Wang, C., Mirshahi, T. and Robishaw, J. D.** (2008). The orphan G protein-coupled receptor 161 is required for left-right patterning. *Dev. Biol.* **323**, 31-40. doi:10.1016/j.ydbio.2008.08.001

**Li, B. I., Matteson, P. G., Ababon, M. F., Nato, A. Q., Lin, Y., Nanda, V., Matise, T. C. and Millonig, J. H.** (2015). The orphan GPCR, Gpr161, regulates the retinoic acid and canonical Wnt pathways during neurulation. *Dev. Biol.* **402**, 17-31. doi:10.1016/j.ydbio.2015.02.007

**Marks, S. A. and Kalderon, D.** (2011). Regulation of mammalian Gli proteins by Costal 2 and PKA in *Drosophila* reveals Hedgehog pathway conservation. *Development* **138**, 2533-2542. doi:10.1242/dev.063479

**Martin, B. R., Deerinck, T. J., Ellisman, M. H., Taylor, S. S. and Tsien, R. Y.** (2007). Isoform-specific PKA dynamics revealed by dye-triggered aggregation and DAKAP1α-mediated localization in living cells. *Chem. Biol.* **14**, 1031-1042. doi:10.1016/j.chembiol.2007.07.017

**Matteson, P. G., Desai, J., Korstanje, R., Lazar, G., Borsuk, T. E., Rollins, J., Kadambi, S., Joseph, J., Rahman, T., Wink, J. et al.** (2008). The orphan G protein-coupled receptor, Gpr161, encodes the vacuolated lens locus and controls neurulation and lens development. *Proc. Natl. Acad. Sci. USA* **105**, 2088-2093. doi:10.1073/pnas.0705657105

**Montague, T. G., Cruz, J. M., Gagnon, J. A., Church, G. M. and Valen, E.** (2014). CHOPCHOP: a CRISPR/Cas9 and TALEN web tool for genome editing. *Nucleic Acids Res.* **42**, W401-W407. doi:10.1093/nar/gku410

**Mukhopadhyay, S., Wen, X., Ratti, N., Loktev, A., Rangell, L., Scales, S. J. and Jackson, P. K.** (2013). The ciliary G-protein-coupled receptor Gpr161 negatively regulates the sonic Hedgehog pathway via cAMP signaling. *Cell* **152**, 210-223. doi:10.1016/j.cell.2012.12.026

**Niewiadomski, P., Kong, J. H., Ahrends, R., Ma, Y., Humke, E. W., Khan, S., Teruel, M. N., Novitch, B. G. and Rohatgi, R.** (2014). Gli protein activity is controlled by multisite phosphorylation in vertebrate Hedgehog signaling. *Cell Rep.* **6**, 168-181. doi:10.1016/j.celrep.2013.12.003

**Niewiadomski, P., Niedziółka, S. M., Markiewicz, Ł., Uśpieński, T., Baran, B. and Chojnowska, K.** (2019). Gli proteins: regulation in development and cancer. *Cells* **8**, 147. doi:10.3390/cells8020147

**Nørholm, M. H. H.** (2010). A mutant Pfu DNA polymerase designed for advanced uracil-excision DNA engineering. *BMC Biotechnol.* **10**, 21. doi:10.1186/1472-6750-10-21

**Ogden, S. K., Fei, D. L., Schilling, N. S., Ahmed, Y. F., Hwa, J. and Robbins, D. J.** (2008). G protein Gαi functions immediately downstream of Smoothened in Hedgehog signalling. *Nature* **456**, 967-970. doi:10.1038/nature07459

**Oldham, W. M. and Hamm, H. E.** (2008). Heterotrimeric G protein activation by G-protein-coupled receptors. *Nat. Rev. Mol. Cell Biol.* **9**, 60-71. doi:10.1038/nrm2299

**Pal, K., Hwang, S.-H., Somatilaka, B., Badgandi, H., Jackson, P. K., DeFea, K. and Mukhopadhyay, S.** (2016). Smoothened determines β-arrestin–mediated removal of the G protein–coupled receptor Gpr161 from the primary cilium. *J. Cell Biol.* **212**, 861-875. doi:10.1083/jcb.201506132

**Pan, Y., Wang, C. and Wang, B.** (2009). Phosphorylation of Gli2 by protein kinase A is required for Gli2 processing and degradation and the Sonic Hedgehog-regulated mouse development. *Dev. Biol.* **326**, 177-189. doi:10.1016/j.ydbio.2008.11.009

**Park, H.-C., Mehta, A., Richardson, J. S. and Appel, B.** (2002). olig2 is required for Zebrafish primary motor neuron and oligodendrocyte development. *Dev. Biol.* **248**, 356-368. doi:10.1006/dbio.2002.0738

**Pusapati, G. V., Kong, J. H., Patel, B. B., Gouti, M., Sagner, A., Sircar, R., Luchetti, G., Ingham, P. W., Briscoe, J. and Rohatgi, R.** (2018). G protein-coupled receptors control the sensitivity of cells to the morphogen sonic Hedgehog. *Sci. Signal.* **11**, eaao5749. doi:10.1126/scisignal.aao5749

**Raleigh, D. R. and Reiter, J. F.** (2019). Misactivation of Hedgehog signaling causes inherited and sporadic cancers. *J. Clin. Investig.* **129**, 465-475. doi:10.1172/JCI120850

**Regard, J. B., Malhotra, D., Gvozdenovic-Jeremic, J., Josey, M., Chen, M., Weinstein, L. S., Lu, J., Shore, E. M., Kaplan, F. S. and Yang, Y.** (2013). Activation of Hedgehog signaling by loss of GNAS causes heterotopic ossification. *Nat. Med.* **19**, 1505-1512. doi:10.1038/nm.3314

**Richardson, K. C., Jarett, L. and Finke, E. H.** (1960). Embedding in epoxy resins for ultrathin sectioning in electron microscopy. *Stain. Technol.* **35**, 313-323. doi:10.3109/10520296009114754

**Riobo, N. A., Saucy, B., DiLizio, C. and Manning, D. R.** (2006). Activation of heterotrimeric G proteins by smoothened. *Proc. Natl. Acad. Sci. USA* **103**, 12607-12612. doi:10.1073/pnas.0600880103

**Ritz, C. and Spiess, A.-N.** (2008). qpcR: an R package for sigmoidal model selection in quantitative real-time polymerase chain reaction analysis. *Bioinformatics* **24**, 1549-1551. doi:10.1093/bioinformatics/btn227

**Röck, R., Mayrhofer, J. E., Torres-Quesada, O., Enzler, F., Raffeiner, A., Raffeiner, P., Feichtner, A., Huber, R. G., Koide, S., Taylor, S. S. et al.** (2019). BRAF inhibitors promote intermediate BRAF(V600E) conformations and binary interactions with activated RAS. *Sci. Adv.* **5**, eaav8463. doi:10.1126/sciadv.aav8463

**Rödiger, S., Burdukiewicz, M., Spiess, A.-N. and Blagodatskikh, K.** (2017). Enabling reproducible real-time quantitative PCR research: the RDML package. *Bioinformatics* **33**, 4012-4014. doi:10.1093/bioinformatics/btx528

**Rstudio Team** (2016). *RStudio: Integrated Development for R* Boston, MA: RStudio, Inc. RStudio.

**Schmitt, E. A. and Dowling, J. E.** (1999). Early retinal development in the zebrafish, *Danio rerio*: light and electron microscopic analyses. *J. Comp. Neurol.* **404**, 515-536. doi:10.1002/(SICI)1096-9861(19990222)404:4<515::AID-CNE8>3.0.CO;2-A

**Schulte-Merker, S. and Stainier, D. Y. R.** (2014). Out with the old, in with the new: reassessing morpholino knockdowns in light of genome editing technology. *Development* **141**, 3103-3104. doi:10.1242/dev.112003

**Shimada, I. S., Hwang, S.-H., Somatilaka, B. N., Wang, X., Skowron, P., Kim, J., Kim, M., Shelton, J. M., Rajaram, V., Xuan, Z. et al.** (2018). Basal suppression of the sonic Hedgehog pathway by the G-protein-coupled receptor Gpr161 restricts medulloblastoma pathogenesis. *Cell Rep.* **22**, 1169-1184. doi:10.1016/j.celrep.2018.01.018

**Singh, J., Wen, X. and Scales, S. J.** (2015). The orphan G protein-coupled receptor Gpr175 (Tpra40) enhances Hedgehog signaling by modulating cAMP levels. *J. Biol. Chem.* **290**, 29663-29675. doi:10.1074/jbc.M115.665810

**Stefan, E., Wiesner, B., Baillie, G. S., Mollajew, R., Kenn, V., Lorenz, D., Furkert, J., Santamaria, K., Nedvetsky, P., Hundsrucker, C. et al.** (2007). Compartmentalization of cAMP-dependent signaling by phosphodiesterase-4D is involved in the regulation of vasopressin-mediated water reabsorption in renal principal cells. *J. Am. Soc. Nephrol.* **18**, 199-212. doi:10.1681/ASN.2006020132

**Stefan, E., Malleshaiah, M. K., Breton, B., Ear, P. H., Bachmann, V., Beyermann, M., Bouvier, M. and Michnick, S. W.** (2011). PKA regulatory subunits mediate synergy among conserved G-protein-coupled receptor cascades. *Nat. Commun.* **2**, 598. doi:10.1038/ncomms1605

**Stückemann, T., Wegleiter, T., Stefan, E., Nägele, O., Tarbashevich, K., Böck, G., Raz, E. and Aanstad, P.** (2012). Zebrafish Cxcr4a determines the proliferative response to Hedgehog signalling. *Development* **139**, 2711-2720. doi:10.1242/dev.074930

**Taylor, S. S., Ilouz, R., Zhang, P. and Kornev, A. P.** (2012). Assembly of allosteric macromolecular switches: lessons from PKA. *Nat. Rev. Mol. Cell Biol.* **13**, 646-658. doi:10.1038/nrm3432

**Thomsen, A. R. B., Plouffe, B., Cahill, T. J., Shukla, A. K., Tarrasch, J. T., Dosey, A. M., Kahsai, A. W., Strachan, R. T., Pani, B., Mahoney, J. P. et al.** (2016). GPCR-G protein-β-arrestin super-complex mediates sustained G protein signaling. *Cell* **166**, 907-919. doi:10.1016/j.cell.2016.07.004

**Torres-Quesada, O., Mayrhofer, J. E. and Stefan, E.** (2017). The many faces of compartmentalized PKA signalosomes. *Cell. Signal.* **37**, 1-11. doi:10.1016/j.cellsig.2017.05.012

**Tschaikner, P., Enzler, F., Torres-Quesada, O., Aanstad, P. and Stefan, E.** (2020). Hedgehog and Gpr161: regulating cAMP signaling in the primary cilium. *Cells* **9**, 118. doi:10.3390/cells9010118

**Tuson, M., He, M. and Anderson, K. V.** (2011). Protein kinase A acts at the basal body of the primary cilium to prevent Gli2 activation and ventralization of the mouse neural tube. *Development* **138**, 4921-4930. doi:10.1242/dev.070805

**Wang, B., Fallon, J. F. and Beachy, P. A.** (2000). Hedgehog-regulated processing of Gli3 produces an anterior/posterior repressor gradient in the developing vertebrate limb. *Cell* **100**, 423-434. doi:10.1016/S0092-8674(00)80678-9

**Whitfield, T. T., Granato, M., van Eeden, F. J., Schach, U., Brand, M., Furutani-Seiki, M., Haffter, P., Hammerschmidt, M., Heisenberg, C. P., Jiang, Y. J. et al.** (1996). Mutations affecting development of the zebrafish inner ear and lateral line. *Development* **123**, 241-254.

**Wickham, H.** (2016). *ggplot2: Elegant Graphics for Data Analysis*. New York: Springer-Verlag.

**Wolff, C., Roy, S. and Ingham, P. W.** (2003). Multiple muscle cell identities induced by distinct levels and timing of Hedgehog activity in the zebrafish embryo. *Curr. Biol.* **13**, 1169-1181. doi:10.1016/S0960-9822(03)00461-5

**Yatsuzuka, A., Hori, A., Kadoya, M., Matsuo-Takasaki, M., Kondo, T. and Sasai, N.** (2019). GPR17 is an essential regulator for the temporal adaptation of sonic Hedgehog signalling in neural tube development. *Development* **146**, dev176784. doi:10.1242/dev.176784

**Yelon, D., Horne, S. A. and Stainier, D. Y. R.** (1999). Restricted expression of cardiac myosin genes reveals regulated aspects of heart tube assembly in zebrafish. *Dev. Biol.* **214**, 23-37. doi:10.1006/dbio.1999.9406

**Zhao, Z., Lee, R. T. H., Pusapati, G. V., Iyu, A., Rohatgi, R. and Ingham, P. W.** (2016). An essential role for Grk2 in Hedgehog signalling downstream of smoothened. *EMBO Rep.* **17**, 739-752. doi:10.15252/embr.201541532